In the Twilight Zone between [2]Pseudorotaxanes and [2]Rotaxanes

Jan O. Jeppesen,*[a, b] Scott A. Vignon,[a] and J. Fraser Stoddart*[a]

Abstract: A [2]pseudorotaxane, based on a semi-dumbbell-shaped component containing asymmetrically substituted monopyrrolotetrathiafulvalene and 1,5-dioxynaphthalene recognition sites for encirclement by cyclobis(paraquat-*p*-phenylene) and with a "speed bump" in the form of a thiomethyl group situated between the two recognition sites, has been self-assembled. This supramolecular entity is a mixture in solution of two slowly interconverting [2]pseudorotaxanes, one of which is on the verge of being a [2]rotaxane at room temperature, allowing it to be isolated by employing flash column chromatography. These two [2]pseudorotaxanes were both characterized in solution by UV/Vis and ^{1}H NMR spectroscopies (1D and 2D) and also by differential pulse voltammetry. The spectroscopic and electrochemical data reveal that one of the complexes behaves wholly as a [2]pseudorotaxane, while the other has some [2]rotaxane character to it. The kinetics of the shuttling of cyclobis(paraquat-*p*-phenylene) between the monopyrrolotetrathiafulvalene and the 1,5-dioxynaphthalene recognition sites have been investigated at different temperatures. The shuttling processes, which are accompanied by detectable color changes, can be monitored using UV/Vis and ^{1}H NMR spectroscopies; the spectroscopic data have been employed in the determination of the rate constants, free energies of activation, enthalpies of activation, and the entropies of activation for the translation of cyclobis(paraquat-*p*-phenylene) between the two recognition sites.

Keywords: electrochemistry · kinetics · rotaxanes · self-assembly · supramolecular chemistry

Introduction

The advent of supramolecular chemistry[1] has aroused the interest of chemists of many different persuasions in exotic compounds such as catenanes and rotaxanes.[2] The synthetic guidance provided by noncovalent bonds has transformed these interlocked molecular compounds from chemical curiosities into the centerpieces of a vibrant area of modern-day research. They are now prime candidates for the construction of artificial molecular machines[3, 4] and the fabrication of nanoelectronic devices.[5–7] Much effort has been devoted to trying to understand and control the use of noncovalent interactions in the template-directed synthesis[8] of catenanes and rotaxanes. A [2]rotaxane is an interlocked molecule composed of a ring and dumbbell-shaped component between which there are no covalent bonds—only a mechanical and noncovalent bonds are present.[2] The ring encircles the linear portion of the dumbbell-shaped component and is trapped mechanically around it by two bulky stoppers. By contrast, in a [2]pseudorotaxane,[2] at least one of the stoppers on the dumbbell-shaped component is absent with the consequence that dissociation into its two components can occur spontaneously. Slipping of macrocycles over the stoppers of dumbbell-shaped components has been used[9] to self-assemble rotaxanes in solution under thermodynamic control. Judicious[9f] choice of the constitution and the size of the slippage stoppers and the macrocycle's cavity are essential in order to reach that fine balance between the system being capable of slippage and not. When such a balance is achieved, the macrocycle possesses sufficient thermal energy in solution, just above room temperature, to permit its slow passage over the stopper. It has been concluded[10] that a well-defined cut-off between rotaxanes and pseudorotaxanes does not exist.[11] In this Paper, we present an example of "piggy-back" supramolecular assistance, which leads to the formation in solution of two [2]pseudorotaxanes, one of which is on the brink of becoming a [2]rotaxane.[12] We have reported previously[13] that slow "internal" passage of cyclobis(paraquat-*p*-phenylene) CBPQT^{4+} over an SMe group occurs (Scheme 1a) in the amphiphilic bistable [2]rotaxane **1**$^{4+}$.

Here, we record the results of kinetic, thermodynamic, and electrochemical studies between a semi-dumbbell-shaped

[a] Dr. J. O. Jeppesen, Prof. J. F. Stoddart, S. A. Vignon
Department of Chemistry and Biochemistry
University of California, Los Angeles
405 Hilgard Avenue, Los Angeles, CA 90095-1569 (USA)
Fax: (+1)310-206-1843
E-mail: joj@chem.sdu.dk, stoddart@chem.ucla.edu

[b] Dr. J. O. Jeppesen
Department of Chemistry
Odense University (University of Southern Denmark)
Campusvej 55, 5230, Odense M (Denmark)
Fax: (+45)66-15-87-80

Supporting information for this article is available on the WWW under http://www.chemeurj.org/or from the author.

 DOI: 10.1002/chem.200304798

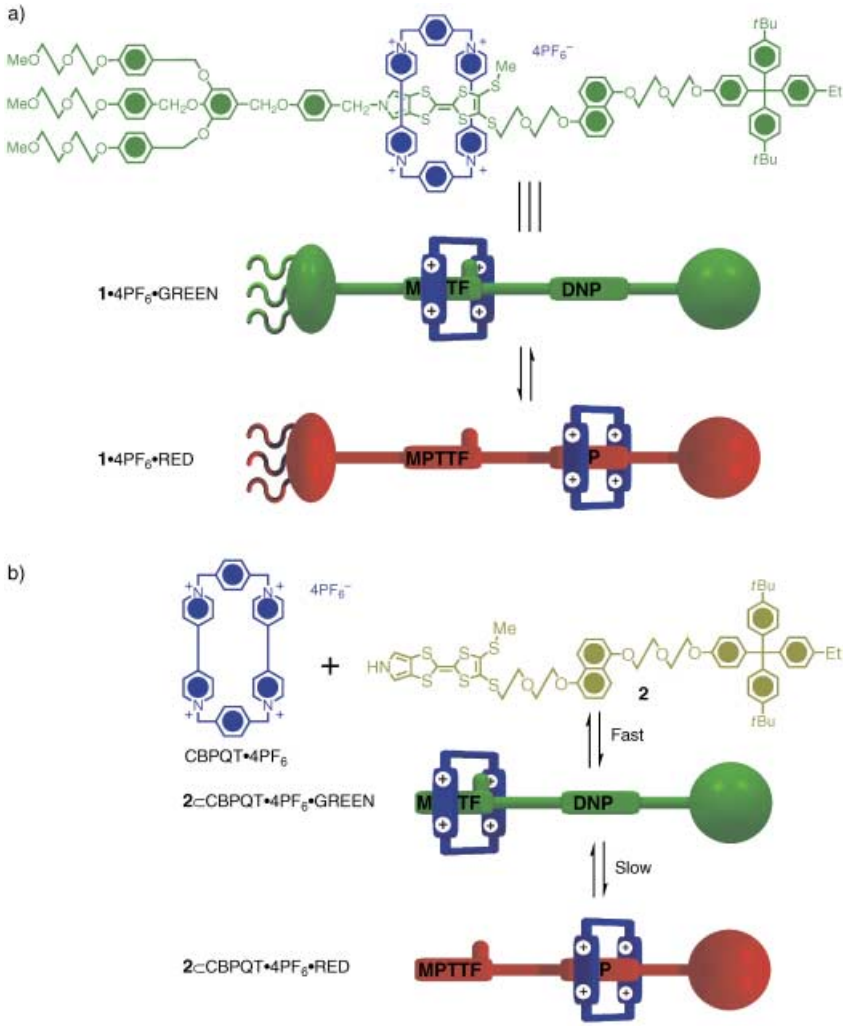

Scheme 1. a) Hindered interconversion in a "slow" bistable amphiphilic [2]rotaxane $\mathbf{1}^{4+}$ and b) self-assembly of the bistable [2]pseudorotaxane $\mathbf{2} \subset$ CBPQT·GREEN^{4+} and its slow interconversion to $\mathbf{2} \subset$ CBPQT·RED^{4+}.

compound **2** and CBPQT^{4+} (Scheme 1b). Compound **2** contains two different recognition sites—a monopyrrolotetrathiafulvalene (MPTTF) one and a 1,5-dioxynaphthalene (DNP) one—for CBPQT^{4+} along with a "speed bump" in the form of an SMe group situated on the rod section between the two recognition sites.

Results and Discussion

Synthesis and photophysical investigations: The inclusion of TTF derivatives inside the cavity of CBPQT^{4+} is well documented[14] and leads to the formation of pseudorotaxanes[2] under thermodynamic control upon mixing of their acyclic and cyclic components in solution. The occurrence of the threading process is evidenced by the ^{1}H NMR and absorption spectra.[14, 15]

Model system: As a model system for $\mathbf{2} \subset$ CBPQT^{4+}, we chose to investigate the complexation (Scheme 2) of CBPQT^{4+} with the semi-dumbbell compound[7d, 16] **3** containing only an MPTTF unit on its rod section. Mixing equimolar proportions of **3** and the tetracationic cyclophane[17] CBPQT^{4+} in Me_2CO or MeCN leads to the formation of the [2]pseudorotaxane $\mathbf{3} \subset$ CBPQT^{4+}, as indicated by the immediate appearance of a green-colored solution; this observation is consistent with a broad charge transfer (CT) band centered on 805 nm in the UV/Vis spectrum (Me_2CO, 298 K), a situation which is characteristic[14] of superstructures containing a TTF unit located inside CBPQT^{4+}. The binding constant (K_a) for the 1:1 complexation of CBPQT^{4+} with **3** has been determined previously[13b] by UV/Vis spectroscopy to be $1300\,\text{M}^{-1}$ ($\varepsilon = 1310\,\text{L mol}^{-1}\,\text{cm}^{-1}$) and $8800\,\text{M}^{-1}$ ($\varepsilon = 1500\,\text{L mol}^{-1}\,\text{cm}^{-1}$) at 298 K in Me_2CO and MeCN, respectively. These K_a values correspond to free energies of complexation[18] ($-\Delta G^\circ$) of 4.2 and 5.4 kcal mol^{-1} at 298 K.

2 $\subset$ *CBPQT*$^{4+}$: Mixing equimolar amounts of the semi-dumbbell compound[13] **2** and CBPQT^{4+} in Me_2CO leads to the formation (Scheme 1b) of $\mathbf{2} \subset$ CBPQT·GREEN^{4+}, as evidenced by the spontaneous production of a green-colored solution. The UV/Vis spectrum (Figure 1a) recorded at 295 K in Me_2CO of this solution showed, immediately after its preparation, a broad band centered on 800 nm as a result of the CT interactions that occur when CBPQT^{4+} encircles[14] the MPTTF unit. Allowing the green solution to stand for 24 h at room temperature produced a brown solution and led (Figure 1c) to a decrease in the intensity of the MPTTF/CBPQT^{4+}

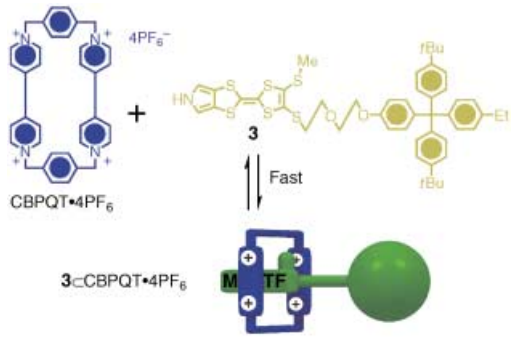

Scheme 2. Complexation of the semi-dumbbell compound **3** by CBPQT^{4+}.

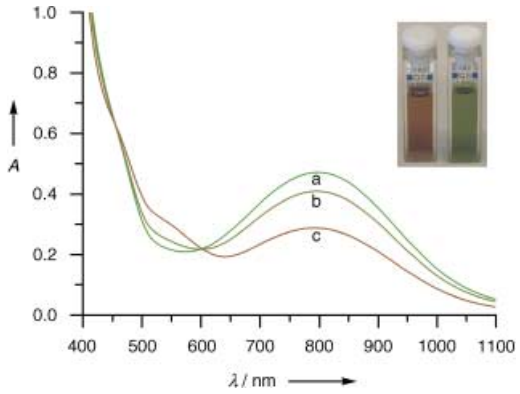

Figure 1. UV/Vis absorption spectra recorded in Me_2CO at 295 K on a 1:1 mixture of **2** and $CBPQT^{4+}$ (0.72 mM) immediately after their mixing (trace a), after 2.5 h (trace b), and after 48 h (trace c). The inset shows the actual colors of the solution immediately after its preparation (green) and after 48 h (brown).

CT band, which was accompanied by the appearance of an absorption band observed as a shoulder at 520 nm that results from the DNP moiety being located inside the cyclophane.[13, 15a, 19] This sequence of events indicates that a partial interconversion of **2**⊂CBPQT·$GREEN^{4+}$ into **2**⊂CBPQT·RED^{4+} has taken place. Thin-layer chromatography (TLC) of the equilibrated brown solution containing **2**⊂CBPQT·$GREEN^{4+}$ and **2**⊂CBPQT·RED^{4+} showed—besides a yellow and a colorless spot arising from **2** and $CBPQT^{4+}$, respectively—only a red spot; this suggests that **2**⊂CBPQT·RED^{4+} may be isolated as a rotaxane-like complex, while **2**⊂CBPQT·$GREEN^{4+}$ dissociates into its components (i.e., **2** and $CBPQT^{4+}$) on the time-scale of the TLC experiment. By employing flash column chromatography, it was possible (Figure 2) to isolate the red co-conformation **2**⊂CBPQT·RED^{4+} in 20% yield,[20] which could be stored for more than

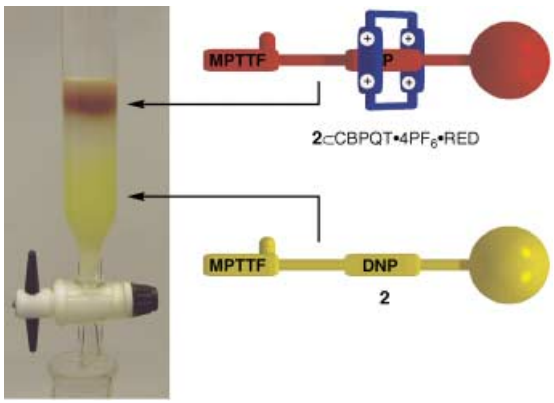

Figure 2. A column chromatogram showing the separation of **2**⊂CBPQT·RED^{4+} from the semi-dumbbell compound **2** and $CBPQT^{4+}$.

two weeks in either Me_2CO or MeCN at −78 °C. The UV/Vis spectrum (Figure 3a) of **2**⊂CBPQT·RED^{4+}, recorded immediately after its isolation in Me_2CO at 296 K, reveals a CT band in the form of a shoulder at 520 nm. It results from the DNP moiety being located inside[13, 15a, 19] $CBPQT^{4+}$. Furthermore, no absorption band is observed in the region 750–850 nm for a CT interaction that would result from the MPTTF unit being located inside the cyclophane,[14] supporting the conclusion that the DNP moiety is encircled exclusively by $CBPQT^{4+}$. Allowing the red solution of **2**⊂CBPQT·RED^{4+} to stand for 24 h at 296 K results in a return to the "original" spectrum (Figure 3c) as a consequence of the passage of $CBPQT^{4+}$ from the DNP to the MPTTF recognition site.

A careful examination of the 800 nm regions in the spectra shown in Figure 1 reveals that the MPTTF/$CBPQT^{4+}$ CT bands of a 1:1 mixture of the semi-dumbbell compound **2** and $CBPQT^{4+}$ immediately after their being mixed and after 48 h have different shapes, with their maxima displaced by 5 nm, an observation which is consistent with the existence in **2**⊂CBPQT·RED^{4+} of folded conformations wherein the MPTTF unit enters into an "alongside" interaction with $CBPQT^{4+}$ in Me_2CO.[21] Further evidence for the existence of such folded conformations comes from the broad CT band observed as a shoulder at 745 nm in the spectrum (Figure 3a) recorded in Me_2CO of **2**⊂CBPQT·RED^{4+}, immediately

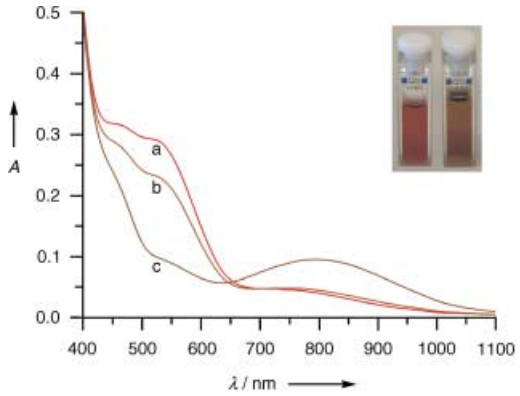

Figure 3. UV/Vis absorption spectra recorded in Me_2CO at 296 K on **2**⊂CBPQT·RED^{4+} (0.28 mM) immediately after its isolation (trace a), after 2.5 h (trace b), and after 48 h (trace c). The inset shows the actual colors of the solution immediately after its isolation (red) and after 48 h (brown).

after its isolation. It can be assigned to the "alongside" MPTTF/$CBPQT^{4+}$ CT interactions. The existence of folded conformations in **2**⊂CBPQT·RED^{4+} seems to be more pronounced in MeCN. Figure 4 illustrates the UV/Vis spectra

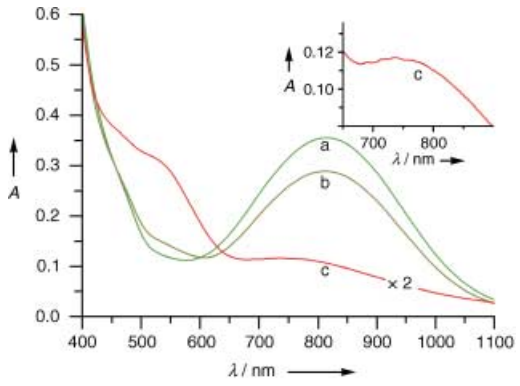

Figure 4. UV/Vis absorption spectra recorded in MeCN at 298 K on a 1:1 mixture of **2** and $CBPQT^{4+}$ (0.20 mM) immediately after their mixture (trace a), after 24 h (trace b), and on **2**⊂CBPQT·RED^{4+} (0.10 mM) immediately after its isolation (trace c).

recorded in MeCN of a 1:1 mixture of **2** and $CBPQT^{4+}$, immediately after their being mixed—and after 24 h and of $\mathbf{2}\subset CBPQT\cdot RED^{4+}$, immediately after its isolation. A comparison of Figures 1 and 4 indicates that the ratio $\mathbf{2}\subset CBPQT\cdot GREEN^{4+}/\mathbf{2}\subset CBPQT\cdot RED^{4+}$ in equilibrated solutions is larger in MeCN than it is in Me_2CO at room temperature. This observation is consistent with the results obtained from ^{1}H NMR spectroscopy (see below). They indicate that, $\mathbf{2}\subset CBPQT\cdot RED^{4+}$ is present in 23 and 35 % in equilibrated CD_3CN and CD_3COCD_3 solutions, respectively. The UV/Vis spectra (Figure 4) recorded on a 1:1 mixture of **2** and $CBPQT^{4+}$ immediately after their being mixed ($\lambda_{max}=$ 817 nm) and after 24 h ($\lambda_{max}=813$ nm) have their maxima displaced by 4 nm, which indicates the existence of folded conformations in $\mathbf{2}\subset CBPQT\cdot RED^{4+}$ in MeCN. The most unequivocal evidence for the existence of folded conformations in $\mathbf{2}\subset CBPQT\cdot RED^{4+}$ in MeCN solution comes from the UV/Vis spectrum recorded of $\mathbf{2}\subset CBPQT\cdot RED^{4+}$ immediately after its isolation. The inset in Figure 4 show the 600–900 nm region of this spectrum and it is clearly evident that an absorption with an ε of about 580 $L\,mol^{-1}\,cm^{-1}$ at $\lambda_{max}=$ 740 nm appears, a feature which can be assigned to the "alongside" MPTTF/$CBPQT^{4+}$ CT interactions. The ε value represents the "average" contribution to the CT interaction from all the possible conformations in which the MPTTF unit is outside the tetracationic cyclophane.[22]

^{1}H NMR investigations: While UV/Vis spectroscopy indicates the position of $CBPQT^{4+}$ on the rod section of the semi-dumbbell component, ^{1}H NMR spectroscopy provides a quantitative tool for monitoring its position and also yields fine, as well as gross, structural information.

Model system: In the case of the 1:1 complex formed between the semi-dumbbell compound **3** and $CBPQT^{4+}$, exchange between the complexed and uncomplexed species occurs rapidly (Figure 5a) on the ^{1}H NMR timescale (CD_3COCD_3, 500 MHz) at 301 K. Thus, the chemical shifts of the observed resonances are the averaged values of those for the complexed and the uncomplexed species. On cooling the CD_3COCD_3 solution down to 194 K, the kinetics enter the regime of slow exchange and both complexed and uncomplexed species can be observed (Figure 5d) in the ^{1}H NMR spectrum of **3** and 1.4 equivalents $CBPQT^{4+}$. In the ^{1}H NMR spectrum recorded (Figure 5c) at 194 K on a 1:1 mixture of **3** and $CBPQT^{4+}$ virtually no uncomplexed $CBPQT^{4+}$ is present, indicating that the complexation of **3** by $CBPQT^{4+}$ is very strong at this temperature. The local asymmetry present in the MPTTF unit is responsible for the desymmetrization of the complexed $CBPQT^{4+}$ ring. It results, for example, in four doublets ($J=6$ Hz) being observed (Figure 5c) for the α-bipyridinium protons in $\mathbf{3}\subset CBPQT^{4+}$.

In order to determine an activation barrier for the complexation/decomplexation process, a CD_3COCD_3 solution of **3** containing 0.70 equivalents of $CBPQT^{4+}$ was studied using variable temperature (VT) ^{1}H NMR spectroscopy. At 290 K, the spectrum (Figure 6a) displayed the expected time-averaged signal for the resonances associated with the protons on the SMe groups. Upon cooling the sample, a gradual broad-

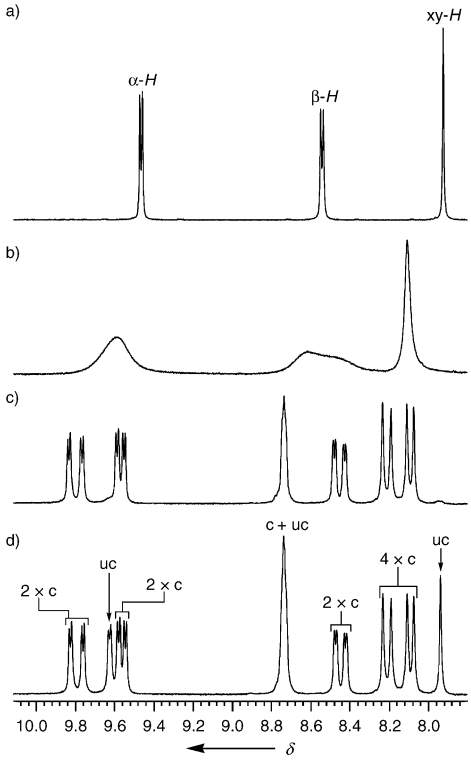

Figure 5. Partial (cyclophane region) ^{1}H NMR spectra (500 MHz) recorded in CD_3COCD_3 of **3** (1.5 mM) and $CBPQT^{4+}$: a) **3**+1.0 equiv $CBPQT^{4+}$ at 301 K, b) **3**+1.0 equiv $CBPQT^{4+}$ at 250 K, c) **3**+1.0 equiv $CBPQT^{4+}$ at 194 K, and d) **3**+1.4 equiv $CBPQT^{4+}$ at 194 K. The descriptions c and uc refer to complexed and uncomplexed $CBPQT^{4+}$ components, respectively.

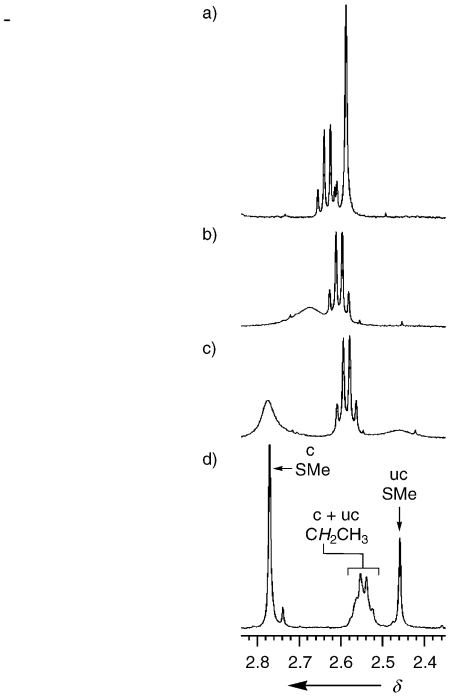

Figure 6. Partial ^{1}H NMR spectra (500 MHz) of the SMe region recorded on a CD_3COCD_3 solution of **3** (1.5 mM)+0.70 equiv $CBPQT^{4+}$ at a) 290 K, b) 247 K, c) 224 K, and d) 194 K. At lower temperatures two signals can be observed for the protons of the SMe group (d). These signals can be attributed to the complexed and uncomplexed forms of **3**. Upon increasing the temperature they are observed to broaden (c) and eventually coalesce into one signal (b) at 247 K. The descriptions c and uc refer to complexed and uncomplexed species, respectively.

ening of this signal occurred, leading eventually to its separation (Figure 6d) into two resonances, which can be associated with the SMe protons in the complexed and uncomplexed forms of **3**. At the coalescence temperature, the activation barrier ($\Delta G_c^{\ddagger}$) for the process, whereby a CBPQT^{4+} ring undergoes exchange between two semi-dumbbell molecules, can be calculated[23] and was determined to be 11.4 ± 0.1 kcal mol^{-1} at 247 K.

2 $\subset$ *CBPQT*$\cdot$ *GREEN*$^{4+}$: In common with the model system, the exchange between the complexed and uncomplexed species in the 1:1 complex formed between **2** and CBPQT^{4+} occurs rapidly on the ^{1}H NMR timescale (CD_3COCD_3, 500 MHz) at 301 K. At 194 K, the kinetics enter the regime of slow exchange. The ^{1}H NMR spectrum recorded (Figure 7b) on a CD_3COCD_3 solution of **2** and 0.66 equivalents of CBPQT^{4+} reveals that only two species are present at 194 K, namely **2** $\subset$ CBPQT$\cdot$GREEN^{4+} and **2**. By contrast, the ^{1}H NMR spectrum recorded (Figure 7c) on a CD_3COCD_3 solution of **2** and 1.04 equivalents of CBPQT^{4+} shows that **2** is completely complexed by CBPQT^{4+}. Hence, **2** $\subset$ CBPQT$\cdot$GREEN^{4+} and CBPQT^{4+} are the only species present in CD_3COCD_3 solution under these conditions. These observations indicate that the complexation of **2** by CBPQT^{4+} is very strong at this temperature. The most diagnostic evidence, which indicates that CBPQT^{4+} encircles the MPTTF unit, is the downfield shift[24] of the resonance for the SMe protons. It is observed (Figure 7c) as a singlet at δ 2.80 for **2** $\subset$ CBPQT$\cdot$GREEN^{4+} compared with a singlet resonating (Figure 7a) at δ 2.49 for uncomplexed **2**. As a consequence of the asymmetry present in the semi-dumbbell component, the DNP-*H*-4/8 protons resonate as two doublets ($J = 8$ Hz) at δ 7.59 and 7.39 and the DNP-*H*-3/7 protons as two triplets ($J = 8$ Hz) centered on δ 7.29 and 7.03, in the spectrum (Figure 8) of **2** $\subset$ CBPQT$\cdot$GREEN^{4+}, while the signals for the DNP-*H*-2/6 protons

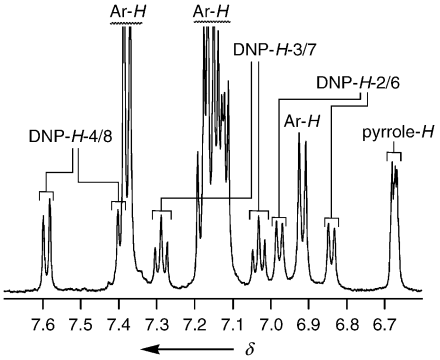

Figure 8. Partial ^{1}H NMR spectrum (500 MHz) recorded in CD_3COCD_3 at 194 K of **2** (1.0 mM)+1.04 equiv CBPQT^{4+}.

resonate as two doublets ($J = 8$ Hz) at δ 6.98 and 6.84. Examination of the ^{1}H DQF-COSY spectrum[25] for **2** $\subset$ CBPQT$\cdot$GREEN^{4+} shows clearly the scalar coupling between the protons in the DNP moiety. The resonances associated with the DNP protons in **2** $\subset$ CBPQT$\cdot$GREEN^{4+} are only slightly upfield shifted (Table 1) as compared to the resonances for the DNP protons in **2**. When a DNP moiety is located "inside" CBPQT^{4+}, the DNP-*H*-4/8 protons resonate[26] at very high field ($\delta = 2.0-3.0$) on account of the [C-H$\cdots\pi$] interactions with the *p*-xylylene units of CBPQT^{4+}. The fact that these DNP protons give rise to signals in the region $\delta = 7.3-7.6$ confirms unequivocally that the DNP moiety is not located inside CBPQT^{4+}.

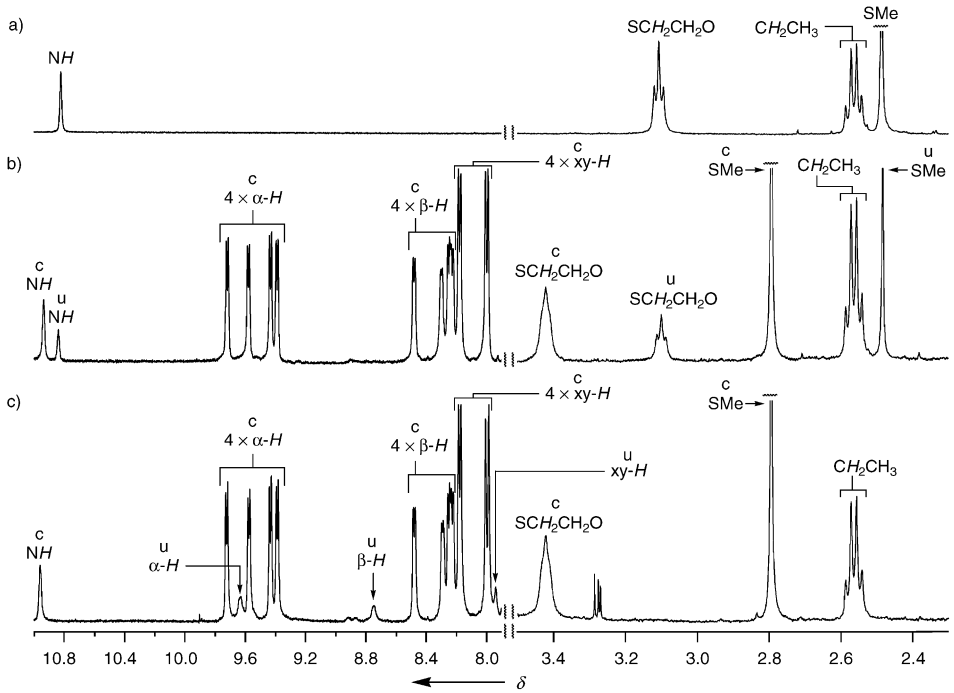

Figure 7. Partial ^{1}H NMR spectra (500 MHz) recorded in CD_3COCD_3 at 194 K of a) **2** (1.5 mM), b) **2** (1.7 mM)+0.66 equiv CBPQT^{4+}, and c) **2** (1.0 mM)+1.04 equiv CBPQT^{4+}. The descriptions c and uc refer to complexed and uncomplexed species, respectively.

2 $\subset$ *CBPQT*$\cdot$ *RED*$^{4+}$: The ^{1}H NMR spectrum (194 K) recorded in CD_3COCD_3 of **2** $\subset$ CBPQT$\cdot$RED^{4+} is shown in Figure 9. Evidence for the fact that CBPQT^{4+} encircles the DNP moiety is apparent from the observation of a high upfield shift (Table 1) of the peaks corresponding to the protons of the DNP moiety. The DNP-*H*-2/6 protons resonate as two doublets ($J = 8$ Hz) at δ 6.34 and 6.35, respectively, in the spectrum (Figure 9) of **2** $\subset$ CBPQT$\cdot$RED^{4+}, while one of the DNP-*H*-3/7 protons resonates as a triplet ($J = 8$ Hz) at δ 6.22. Although the signal for the other DNP-*H*-3/7 proton is obscured by the multiplet for the $^+$NC*H*$_2$ protons, it is clearly evident in the ^{1}H DQF-COSY spectrum[25] and resonates at δ 6.20. The upfield shift of the

Table 1. Selected ^{1}H NMR spectroscopic data[a] (δ values) for **2**, CBPQT^{4+}, **2** $\subset$ CBPQT$\cdot$GREEN^{4+}, and **2** $\subset$ CBPQT$\cdot$RED^{4+} in CD_3COCD_3 at 194 K. s = singlet, d = doublet, t = triplet, m = multiplet, brs = broad singlet, and brt = broad triplet.

	Semi-dumbbell **2**	CBPQT^{4+}	**2** $\subset$ CBPQT$\cdot$GREEN^{4+}	**2** $\subset$ CBPQT$\cdot$RED^{4+}
N*H*	10.82 (s)	–	10.96 (s)	10.69 (s)
α-*H*	–	9.65 (d)	9.72 (d), 9.57 (d), 9.43 (d), 9.39 (d)	9.45 (d), 9.36 (d), 9.19 (d), 9.14 (d)
β-*H*	–	8.76 (d)	8.48 (d), 8.29 (d), 8.25 (d), 8.23 (d)	7.88 (d), 7.86 (d), 7.73 (d),[b] 7.63 (d)[b]
Xy-*H*	–	7.95 (s)	8.19 (s), 8.17 (s), 8.01 (s), 7.98 (s)	8.45 (s), 8.43 (s), 8.23 (s), 8.21 (s)
DNP-*H*-4/8	7.83 (d), 7.80 (d)	–	7.59 (d), 7.39 (d)	2.62 (d), 2.60 (d)
DNP-*H*-3/7	7.42 (t), 7.36 (t)	–	7.29 (t), 7.03 (t)	6.22 (t), 6.20 (t)[b]
DNP-*H*-2/6	6.99 (d), 6.97 (d)	–	6.98 (d), 6.84 (d)	6.35 (d), 6.34 (d)
pyrrole-*H*	6.95 – 6.97 (m)	–	6.67 – 6.69 (m)	6.74 (brs), 6.64 (brs)
SCH_2SCH_2	3.11 (t)	–	3.42 (brt)	3.48 (brt)
SMe	2.49 (s)	–	2.80 (s)	2.53 (s)

[a] ^{1}H NMR spectra were recorded at 500 MHz. [b] Identified from the ^{1}H DQF-COSY spectrum.

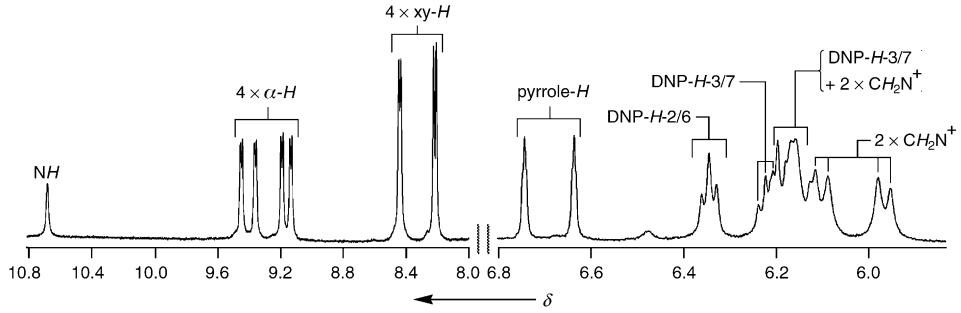

Figure 9. Partial ^{1}H NMR spectrum (500 MHz) of isolated **2** $\subset$ CBPQT$\cdot$RED^{4+} ($\approx$2 mM) recorded in CD_3COCD_3 at 194 K (the peaks for the DNP-*H*-4/8 protons appear at δ 2.60 and 2.62 and are not shown here).

DNP-*H*-2/6 and DNP-*H*-3/7 protons results from anisotropic shielding of the protons on the DNP moiety by the aromatic units present in the encircling CBPQT^{4+} ring. Additionally, the DNP-*H*-4/8 protons of the encircled DNP moiety participate in [C-H$\cdots\pi$] interactions. The fact that they are pointing toward the π faces of the *p*-xylylene units of CBPQT^{4+} results in a very large upfield shift of their resonances, which are observed as two doublets (J = 8 Hz) at δ 2.60 and 2.62. The δ values for the DNP-*H*-4/8 protons in **2** $\subset$ CBPQT$\cdot$RED^{4+} and the same protons in **2** are shifted upfield by 5.21 and 5.20 ppm. The ^{1}H DQF-COSY spectrum[25] recorded on **2** $\subset$ CBPQT$\cdot$RED^{4+} shows the scalar coupling between the protons in the DNP moiety. No signals corresponding to an uncomplexed DNP moiety are observed for the isolated **2** $\subset$ CBPQT$\cdot$RED^{4+}, indicating that the DNP moiety is completely encircled by CBPQT^{4+}, at least within the limits of detection in these experiments.

Equilibrated solutions: The ^{1}H NMR spectra (273 K) recorded on equilibrated Me_2CO (1.0 mM) or MeCN (0.80 mM) solutions, containing initially a 1:1 mixture of **2** and CBPQT^{4+}, revealed that these solutions contained 35 and 23%, respectively, of **2** $\subset$ CBPQT$\cdot$RED^{4+}.[27]

Dynamic and kinetic investigations: A fundamental understanding of the shuttling behavior in solution by bistable [2]rotaxanes must be achieved if their switching properties in solid-state devices[7] are going to be harnessed to the full. Toward this end, a detailed kinetic investigation of the shuttling behavior of the tetracationic ring component between the two recognition sites in **2** $\subset$ CBPQT^{4+} has been carried out with the objective of obtaining the thermodynamic parameters for the process. The kinetics of the movement of CBPQT^{4+} between the MPTTF and the DNP recognition sites were investigated in Me_2CO and MeCN, using UV/Vis spectroscopy as the probe. This shuttling process is a unimolecular reaction and can accordingly be expected to follow first-order kinetics.[28]

GREEN to RED: The first-order kinetics for the process whereby CBPQT^{4+} moves from the MPTTF to the DNP recognition site in **2** $\subset$ CBPQT^{4+} were investigated by monitoring the increase in the CT band intensity resulting from the DNP moiety being located inside CBPQT^{4+}. Immediately after mixing equimolar amounts of CBPQT^{4+} and **2** in Me_2CO,[20] a UV/Vis spectrum was recorded and the movement of CBPQT^{4+} from the MPTTF to the DNP recognition site was followed at different temperatures (Table 2) using the DNP/CBPQT^{4+} CT band (520 nm) as the probe. After 24 h, all the equilibrating systems had reached equilibrium and no perceptible changes were observed in UV/Vis spectra recorded subsequently. The experimental data were subjected to a first-order analysis and rate constants (k) were obtained for the passage of CBPQT^{4+} over the SMe group in the direction from **2** $\subset$ CBPQT$\cdot$GREEN^{4+} to **2** $\subset$ CBPQT$\cdot$RED^{4+} in Me_2CO at different temperatures. The straight lines obtained by plotting $\ln A/A_0$ against time (t) confirm[29] the first-order nature of the shuttling process. The k values and the corresponding free energies of activation[30] ($\Delta G^{\ddagger}$) were obtained directly from the slopes of these straight lines and are recorded in Table 2, together with the half-lifes ($t_{1/2}$) for this co-conformational change. Since the MPTTF/CBPQT^{4+} CT band intensities also show (Figure 1) significant changes as time progresses, it might be expected that this band could also be used as a probe for monitoring the passage of CBPQT^{4+}

Table 2. Rate constants (k) and derived free energies of activation[30] ($\Delta G^{\neq}$) for the slippage of $CBPQT^{4+}$ over the SMe group in **2** in the direction from GREEN to RED determined by UV/Vis spectroscopy in Me_2CO[a] at different temperatures using the DNP/$CBPQT^{4+}$ CT band as probe.

T [K]	λ_{max} [nm]	Data points	Correlation coefficient	k [s^{-1}]	$t_{1/2}$ [min][b]	$\Delta G^{\neq}$ [kcal mol^{-1}]
292	520	13	0.998	1.4×10^{-5}	830	23.5
295	520	10	0.990	1.9×10^{-5}	610	23.6
297	520	15	0.995	2.6×10^{-5}	440	23.6
301	520	12	0.996	3.6×10^{-5}	320	23.7
305	520	8	0.992	4.8×10^{-5}	240	23.8
308	520	8	0.998	6.9×10^{-5}	170	23.9

[a] Experiments were performed with an initial concentration of **2** (equal to that of $CBPQT^{4+}$) of 0.72 mM. The k values were obtained from the slope of the straight line in the plot of $\ln A/A_0$ against t using the relationship of $\ln A/A_0 = -kt$. The values A and A_0 correspond to the absorbance (at 520 nm) at time t and A_0 to the initial absorbance (at 520 nm), respectively. [b] The values of "half-life" quoted were obtained from $t_{1/2} = \ln 2/k$ and are the theoretical values that would be observed in a nonequilibrating system, i.e., if the reverse process was prevented by constant removal of the separated components from the system.

Table 3. Rate constants (k) and derived free energies of activation[30] ($\Delta G^{\neq}$) for the slippage of $CBPQT^{4+}$ over the SMe group in **2** in the direction from RED to GREEN determined by UV/Vis spectroscopy in Me_2CO[a] at different temperatures using the DNP/$CBPQT^{4+}$ CT band as probe.

T [K]	λ_{max} [nm]	Data points	Correlation coefficient	k [s^{-1}]	$t_{1/2}$ [min][b]	$\Delta G^{\neq}$ [kcal mol^{-1}]
295	520	17	0.999	1.4×10^{-5}	830	23.8
297	520	15	0.999	1.9×10^{-5}	610	23.8
301	520	13	0.999	2.7×10^{-5}	430	23.9
305	520	13	0.999	3.9×10^{-5}	300	24.0
309	520	17	0.999	5.5×10^{-5}	210	24.1
312	520	15	1.000	7.6×10^{-5}	150	24.2

[a] Experiments were performed with an initial concentration of **2**$\subset$ $CBPQT\cdot RED^{4+}$ of 0.19 mM. The Me_2CO solution of **2**$\subset CBPQT\cdot RED^{4+}$ also contained small amounts of NH_4PF_6. The k values were obtained from the slope of the straight line in the plot of $\ln A/A_0$ against t using the relationship of $\ln A/A_0 = -kt$. The values A and A_0 correspond to the absorbance (at 520 nm) at time t and A_0 to the initial absorbance (at 520 nm), respectively. [b] The values of "half-life" quoted were obtained from $t_{1/2} = \ln 2/k$ and are the theoretical values that would be observed in a nonequilibrating system, i.e., if the reverse process was prevented by constant removal of the separated components from the system.

over the SMe group. However, as a consequence of the existence of folded semi-dumbbell conformations (see above) in **2**$\subset CBPQT\cdot RED^{4+}$, the decrease in the CT band ($\lambda_{max} =$ 800 nm) associated with the MPTTF unit located "inside" $CBPQT^{4+}$ in **2**$\subset CBPQT\cdot GREEN^{4+}$ is accompanied by an increase in the CT band ($\lambda_{max} = 740$ nm) caused by the MPTTF unit entering into an "alongside" interaction with $CBPQT^{4+}$ in **2**$\subset CBPQT\cdot RED^{4+}$. Therefore, it is not feasible to use the absorption band at 800 nm as a probe for monitoring the shuttling of $CBPQT^{4+}$ between the MPTTF unit and the DNP moiety.[31, 32]

RED to GREEN: The first-order kinetics for the process whereby $CBPQT^{4+}$ moves from the DNP to the MPTTF recognition site of **2**$\subset CBPQT^{4+}$ were investigated by monitoring the decrease in the CT band intensities resulting from the DNP moiety being located inside $CBPQT^{4+}$. Immediately after isolation of **2**$\subset CBPQT\cdot RED^{4+}$, UV/Vis spectra were recorded[20] in both Me_2CO and MeCN. The passage of $CBPQT^{4+}$ from the DNP to the MPTTF recognition site was followed at different temperatures (Tables 3 and 4), using the DNP/$CBPQT^{4+}$ CT band (520 nm) as the probe. After 24 h, the equilibrating systems reached equilibrium and no perceptible changes were observed in UV/Vis spectra recorded subsequently. As a consequence of the spectroscopic changes, the color of the solutions changes from red to brown (inset in Figure 3). On carrying out a first-order kinetic analysis,[29] rate constants for the passage of $CBPQT^{4+}$ over the SMe group in the direction from **2**$\subset CBPQT\cdot RED^{4+}$ to **2**$\subset CBPQT\cdot GREEN^{4+}$ were obtained (Tables 3 and 4) at different temperatures in both Me_2CO and MeCN. Figure 10 shows the linear plots of $\ln A/A_0$ against t for the slippage of $CBPQT^{4+}$ over the SMe group in **2** in the direction from the DNP moiety to the MPTTF unit in Me_2CO at different temperatures. The rate constants and the corresponding $\Delta G^{\neq}$ values,[30] obtained from these UV/Vis experiments, are recorded in Tables 3 and 4 together with the $t_{1/2}$ values for this co-conformational change.[33]

Table 4. Rate constants (k) and derived free energies of activation[30] ($\Delta G^{\neq}$) for the slippage of $CBPQT^{4+}$ over the SMe group in **2** in the direction from RED to GREEN determined by UV/Vis spectroscopy in MeCN[a] at different temperatures using the DNP/$CBPQT^{4+}$ CT band as probe.

T [K]	λ_{max} [nm]	Data points	Correlation coefficient	k [s^{-1}]	$t_{1/2}$ [min][b]	$\Delta G^{\neq}$ [kcal mol^{-1}]
293	520	13	0.999	2.3×10^{-5}	500	23.3
295	520	14	0.997	3.1×10^{-5}	370	23.4
298	520	17	0.998	4.2×10^{-5}	280	23.4
300	520	8	0.996	5.3×10^{-5}	220	23.4
302	520	8	0.997	6.5×10^{-5}	180	23.5
306	520	8	0.999	9.8×10^{-5}	120	23.5

[a] Experiments were performed with an initial concentration of **2**$\subset$ $CBPQT\cdot RED^{4+}$ of 0.10 mM. The MeCN solution of **2**$\subset CBPQT\cdot RED^{4+}$ also contained small amounts of NH_4PF_6. The k values were obtained from the slope of the straight line in the plot of $\ln A/A_0$ against t using the relationship of $\ln A/A_0 = -kt$. The values A and A_0 correspond to the absorbance (at 520 nm) at time t and A_0 to the initial absorbance (at 520 nm), respectively. [b] The values of "half-life" quoted were obtained from $t_{1/2} = \ln 2/k$ and are the theoretical values that would be observed in a nonequilibrating system, i.e., if the reverse process was prevented by constant removal of the separated components from the system.

Thermodynamic parameters: Since, the $\Delta G^{\neq}$ values have been determined at different temperatures the enthalpic ($\Delta H^{\neq}$) and entropic ($\Delta S^{\neq}$) contributions to the shuttling process can be calculated from a plot (Figure 11) of $\Delta G^{\neq}$ against T. In addition, an Arrhenius plot[25] gives the activation energy (E_a) and the pre-exponential factor (A). The kinetic parameters obtained from these plots are summarized in Table 5.[34]

Discussion of kinetic and thermodynamic parameters: Knowledge of the thermodynamic parameters associated with the shuttling processes between the MPTTF and DNP recognition sites at room temperature is of crucial importance in view of the use of these supramolecular entities in the fabrication of devices. It is evident from inspection of the data in Table 5

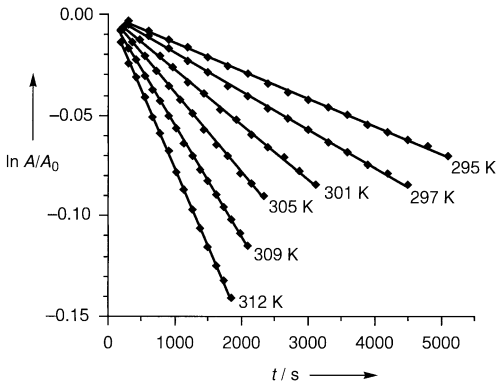

Figure 10. Linear plots of $\ln A/A_0$ against t for the slippage of CBPQT^{4+} over the SMe group in **2** in the direction from RED to GREEN in Me_2CO at different temperatures obtained by using the DNP/CBPQT^{4+} CT absorption band (520 nm) as probe. The data points were collected in the early stage of the experiments where the reverse process is not yet occurring to any significant extent and have been fitted by best straight lines, giving correlation coefficients of 0.999 – 1.000, indicating that first-order kinetics are in operation. The slope of each line give the k value, according to the relationship $\ln A/A_0 = -kt$.

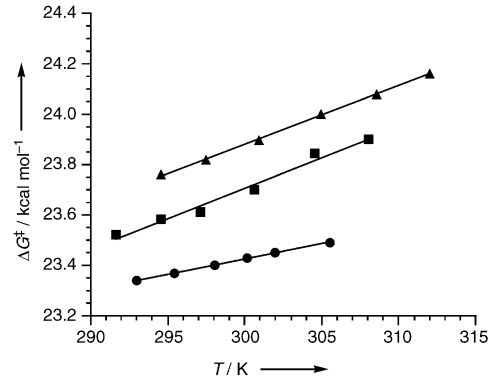

Figure 11. Linear plots of ΔG^{+} against T for the slippage of CBPQT^{4+} over the SMe group in **2** in the direction from GREEN to RED in Me_2CO (■), in the direction from RED to GREEN in Me_2CO (▲), and in the direction from RED to GREEN in MeCN (●). The ΔG^{+} values were obtained as described in Tables 2 – 4. The slope and intercept of each line of best fit give the values ΔS^{+} and ΔH^{+} (see Table 5), respectively, from the equation $\Delta G^{+} = \Delta H^{+} - T\cdot\Delta S^{+}$.

that the passage of CBPQT^{4+} over the SMe group is a significantly faster process in MeCN than it is in Me_2CO at room temperature. In fact, the free energy of activation is 0.4 kcal mol^{-1} lower in the former than it is in the latter. Although, the enthalpies of activation are positive in both solvents, the ΔH^{+} value is approximately 3 kcal mol^{-1} higher in MeCN than it is in Me_2CO. A much more pronounced difference is evident when the entropies of activation for the passage of CBPQT^{4+} over the SMe group in these two solvents are compared. Although the ΔS^{+} value is negative in both solvents, the value is twice as large in Me_2CO than it is in MeCN; this indicates that the passage of CBPQT^{4+} over the SMe group is much more dominated by a loss of entropy in the transition state in the case of Me_2CO. The entropy of activation ΔS^{+} is related to two major factors.[11b] 1) A loss of translational, rotational, and vibrational degrees of freedom on the part of CBPQT^{4+} upon its expanding to pass over the SMe group would contribute negatively to the total entropy of activation in both solvents. 2) A change in the solvation of the semi-dumbbell-shaped component when the ring component migrates from the recognition sites to the SMe group would also affect the entropy of activation. The solubility of the semi-dumbbell component is much higher (>20 times) in Me_2CO than it is in MeCN. The aromatic surfaces of the DNP and MPTTF recognition sites become more exposed to the solvent when they are not engaged in donor – acceptor interactions with CBPQT^{4+}, that is, the rotaxane-like complex is less polar at the transition state than it is when the ring component encircles one of the two recognition sites. As a direct consequence of the higher solubility of the semi-dumbbell component in Me_2CO, and the fact that Me_2CO (dielectric constant, $\varepsilon = 20.7$) is less polar than MeCN ($\varepsilon = 37.5$), the Me_2CO solvent molecules are more ordered around the aromatic surfaces of the DNP and MPTTF recognition sites in the transition state than they are in the ground states of **2** ⊂ CBPQT^{4+}. Thus, the entropy of solvation takes on a more negative value in Me_2CO than in MeCN. If it is assumed that the negative effect of the loss of freedom of motion of the CBPQT^{4+} ring component is the same in Me_2CO and MeCN, the result will be a total entropy of activation which is more negative in Me_2CO than it is in MeCN.

Electrochemical investigations: These were carried out in nitrogen-purged MeCN solutions at room temperature using cyclic voltammetry (CV) and differential pulse voltammetry (DPV). Our studies have been focussed on the oxidation processes of the MPTTF units contained in the semi-dumbbell components.

Semi-dumbbells: The semi-dumbbell compounds **3** and **2** contain, respectively, one (MPTFF) or two (MPTTF and DNP) electron-donating units and one stopper, incorporating

Table 5. Kinetic and thermodynamic parameters for the passage of CBPQT^{4+} over the SMe group in **2** at 297 K.

	Solvent	k[a] [s^{-1}]	$t_{1/2}$[a] [min]	ΔG^{+} (297 K)[a] [kcal mol^{-1}]	ΔH^{+}[b] [kcal mol^{-1}]	ΔS^{+}[b] [cal mol^{-1} K^{-1}]	E_a[c] [kcal mol^{-1}]	A[c] [s^{-1}]
GREEN to RED	Me_2CO	2.6×10^{-5}	440	23.6	16.4	−24	17.6	150×10^{6}
RED to GREEN	Me_2CO	1.9×10^{-5}	610	23.8	17.0	−23	17.1	88×10^{6}
RED to GREEN	MeCN	4.2×10^{-5}[d]	280	23.4	19.8	−12	20.4	$37\,600\times10^{6}$

[a] The k, $t_{1/2}$, and ΔG^{+} values were obtained as described in Tables 2 – 4 and the estimated errors are ±5%. [b] The ΔH^{+} and ΔS^{+} values were obtained from the intercept and slope of the straight line in the plot of ΔG^{+} against T using the relationship $\Delta G^{+} = \Delta H^{+} - T\cdot\Delta S^{+}$, where T is the absolute temperature; the estimated errors are ±5% for ΔH^{+} and ±25% for ΔS^{+}. [c] The E_a and A values were obtained from the intercept and slope of the straight line in the plot of $\ln k$ against T^{-1} using the relationship $\ln k = \ln A - (E_a/R)(T^{-1})$, where R is the gas constant and T is the absolute temperature; the estimated errors are ±5% for E_a and ±25% for A. [d] At 298 K.

phenoxy units, which are also expected to exhibit some electron-donating ability.[8g, 35] Compounds **2** and **3** both show[25] two reversible, monoelectronic oxidation processes, associated with the MPTTF unit. A comparison of the results obtained (Table 6) shows that both the first and the second oxidation processes associated with the MPTTF unit in **2** take place at a potential that is less positive than these observed for **3**. This behavior can be attributed to the presence of stabilizing interactions between both the $MPTTF^{+\bullet}$ and $MPTTF^{2+}$ and the DNP moiety[13b, 36] present in **2**.

Table 6. Electrochemical data[a] for **3**, **2**, **3**$\subset$CBPQT^{4+}, **2**$\subset$CBPQT·GREEN^{4+}, and **2**$\subset$CBPQT·RED^{4+}.

	MPTTF[b]	
Compound/Complex	E_{ox}^1 [V][c]	E_{ox}^2 [V][c]
3	+0.44	+0.74
2	+0.41	+0.72
3$\subset$CBPQT^{4+}	+0.48	+0.74
2$\subset$CBPQT·GREEN^{4+}	+0.45	+0.72
2$\subset$CBPQT·RED^{4+}	+0.50	+0.77

[a] Nitrogen-purged MeCN, room temperature and tetrabutylammonium hexafluorophosphate ($TBAPF_6$) as supporting electrolyte, platinum disk as working electrode. [b] Unit involved in the observed processes. [c] Potential values in V vs SCE; reversible and monoelectronic processes.

Model system: A binding constant[13b] of 8800 M^{-1} (MeCN, 298 K) for the complexation between CBPQT^{4+} and **3** is not large enough to avoid the presence of substantial amounts of free species when equimolar concentrations in the range of 0.01 to 1 mM of the two components are present in MeCN solutions. For this reason, the electrochemical investigation of **3**$\subset$CBPQT^{4+} was carried out in a MeCN solution containing 0.1 mM of **3** and an excess (10 equivalents) of CBPQT^{4+}. Under these conditions,[37] the fraction (89%) of **3**$\subset$CBPQT^{4+} is very large compared with the small amount of uncomplexed **3**. It has been possible, therefore, to study the oxidation of the MPTTF unit engaged in this [2]pseudorotaxane. The results obtained (Table 6) for **3** and **3**$\subset$CBPQT^{4+} show that, in **3**$\subset$CBPQT^{4+}, the first oxidation of the MPTTF unit displays a small anodic shift (40 mV) when compared to that for **3**, whereas the second oxidation potential is unaffected by the presence of CBPQT^{4+}. These results can be explained[38] as follows. 1) In **3**$\subset$CBPQT^{4+}, the MPTTF unit is engaged in CT interactions with CBPQT^{4+} while 2), after the first oxidation of the MPTTF unit, dethreading takes place because the noncovalent interactions between the $MPTTF^{+\bullet}$ unit and CBPQT^{4+} are eradicated and a Coulombic repulsion is introduced between the mono-oxidized $MPTTF^{+\bullet}$ unit and the tetracationic cyclophane. Consequently 3), the second oxidation of the $MPTTF^{+\bullet}$ unit in the mixture of uncomplexed $\mathbf{3}^{+\bullet}$ and uncomplexed CBPQT^{4+} takes place at the same potential as that of the second oxidation of the semi-dumbbell component.

2 $\subset$ *CBPQT·GREEN*$^{4+}$: Although the binding constant between **2** and CBPQT^{4+} has not been determined, it is expected to have a magnitude which is, at least, not smaller than the K_a value for the complexation of CBPQT^{4+} with **3**. As before, the electrochemical investigations of **2**$\subset$CBPQT·GREEN^{4+} were carried out in a MeCN solution containing the semi-dumbbell component and an excess of CBPQT^{4+} in order to avoid the presence of substantial amounts of free species. The electrochemical data[25] for **2**$\subset$CBPQT·GREEN^{4+} were obtained in a MeCN solution containing **2** (0.2 mM) and 10 equivalents of CBPQT^{4+} immediately after its preparation.[39] A comparison (Table 6) of the results obtained for **2** and **2**$\subset$CBPQT·GREEN^{4+} show that, in **2**$\subset$CBPQT·GREEN^{4+}, the first oxidation of the MPTTF unit is shifted (40 mV) towards more positive potentials with respect to that of **2**, while the second oxidation takes place at the same potential for both **2** and its 1:1 complex. These results are similar to those obtained for **3**$\subset$CBPQT^{4+} and indicate that **2**$\subset$CBPQT·GREEN^{4+} behaves electrochemically like a [2]pseudorotaxane, that is, dethreading takes place after the first oxidation of the MPTTF unit in the semi-dumbbell component.

Allowing the MeCN solution of **2**$\subset$CBPQT·GREEN^{4+} to stand for 24 h at room temperature produced a greenish brown solution and led[25] to anodic shifts of both the first and second oxidation potentials in comparison with the first and second oxidation process in **2**$\subset$CBPQT·GREEN^{4+}. Moreover, these anodic shifts were accompanied by both a decrease in the current intensities and a broadening of the DPV peaks. These observations can be explained by the partial interconversion of **2**$\subset$CBPQT·GREEN^{4+} into **2**$\subset$CBPQT·RED^{4+} that takes place in the MeCN solution. Both the first and the second oxidations of **2**$\subset$CBPQT·RED^{4+} take place (Table 6) at slightly higher potentials (50 mV), than those of **2**$\subset$CBPQT·GREEN^{4+}. Therefore, the peak observed[25] at +0.47 V can be assigned to the overlapping of the first oxidation process of the MPTTF unit in **2**$\subset$CBPQT·GREEN^{4+} and the first oxidation process of the MPTTF unit in **2**$\subset$CBPQT·RED^{4+}, whereas the peak observed[25] at +0.73 V arises from the overlapping of the second oxidation process of the MPTTF unit in **2**$\subset$CBPQT·GREEN^{4+} and the second oxidation process of the MPTTF unit in **2**$\subset$CBPQT·RED^{4+}.

2 $\subset$ *CBPQT·RED*$^{4+}$: The electrochemical characterization of **2**$\subset$CBPQT·RED^{4+} was carried out on a MeCN solution containing 0.10 mM of **2**$\subset$CBPQT·RED^{4+}, prepared immediately after its isolation. Since, **2**$\subset$CBPQT·RED^{4+} was isolated as a rotaxane-like complex, the semi-dumbbell component and ring component are present in a 1:1 ratio. This situation is in contrast to the electrochemical investigations performed on **2**$\subset$CBPQT·GREEN^{4+}, which were carried out on a solution of **2** and 10 equivalents of CBPQT^{4+}. The results obtained (Figure 12a and Table 6) for **2**$\subset$CBPQT·RED^{4+}, prepared immediately after its isolation, show that both the first and second oxidations of the MPTTF unit are shifted towards considerably more positive potentials—by 90 and 40 mV, respectively—with respect to those of **2**. The large anodic shift of the first oxidation potential cannot be explained solely by the unfavorable Coulombic repulsion, arising between the mono-oxidized $MPTTF^{+\bullet}$ unit and CBPQT^{4+} encircling the DNP moiety. The photophysical investigations indicate (see above) that the MPTTF unit in

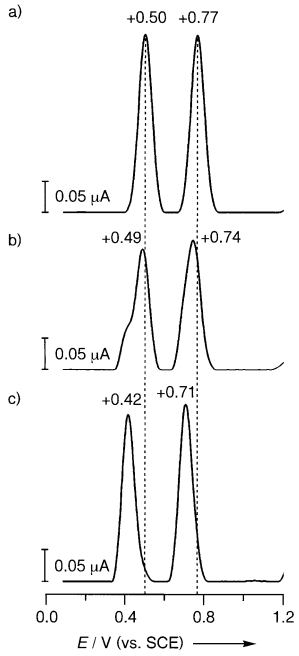

Figure 12. Differential pulse voltammograms (DPVs) recorded in MeCN at 298 K on a) $\mathbf{2}\subset$CBPQT$\cdot$RED^{4+} (0.1 mM) immediately after its isolation, b) after 3 h, and c) after 24 h.

$\mathbf{2}\subset$CBPQT$\cdot$RED^{4+} is engaged in "alongside" interactions with CBPQT^{4+} as expressed (Scheme 3) by the presence of folded superstructures. We can thus associate the process at +0.50 V with the first oxidation of the MPTTF unit which is interacting in an "alongside" manner with CBPQT^{4+}. Removal of one electron (MPTTF $\rightarrow$ MPTTF$^{+\cdot}$) from such folded conformations results in the breaking of the favorable donor–acceptor interactions between the MPTTF unit and the bipyridinium units in CBPQT^{4+}, leading to unfolding of the pseudorotaxane. Reduction (MPTTF$^{+\cdot}$ $\rightarrow$ MPTTF) of the mono-oxidized MPTTF$^{+\cdot}$ unit to its neutral form regenerates the "linear" conformation of $\mathbf{2}\subset$CBPQT$\cdot$RED^{4+}, which is in equilibrium with its folded conformations. The shift of 40 mV toward more positive potentials for the second oxidation process in $\mathbf{2}\subset$CBPQT$\cdot$RED^{4+}, compared with the same process for **2**, can be explained by the formation of further Coulombic repulsion between the di-oxidized MPTTF^{2+} unit and the electron-accepting CBPQT^{4+}.

The conversion of $\mathbf{2}\subset$CBPQT$\cdot$RED^{4+} into $\mathbf{2}\subset$CBPQT$\cdot$GREEN^{4+} could be followed by monitoring the changes in the positions and the shapes of the DPV peaks. Figure 12b shows the DPV recorded on a solution of $\mathbf{2}\subset$CBPQT$\cdot$RED^{4+} 3 h after its isolation. A comparison of the DPV peaks in Figure 12a and b reveal anodic shifts, decreases in the current intensities, and broadening of the DPV peaks, all indicating that these peaks can be attributed to the overlapping of oxidation processes from three different species, namely, **2**, $\mathbf{2}\subset$CBPQT$\cdot$GREEN^{4+}, and $\mathbf{2}\subset$CBPQT$\cdot$RED^{4+}. After 24 h at room temperature, the system had equilibrated and no perceptible changes were observed in the voltammograms recorded (Figure 12c) subsequently. Assuming that the K_a value for the complexation of **2** by CBPQT^{4+} is approximately the same as that for the complexation between CBPQT^{4+} and **3** and, since the electrochemical investigations of $\mathbf{2}\subset$CBPQT$\cdot$RED^{4+} were carried out on a MeCN solution containing initially 0.10 mM of $\mathbf{2}\subset$CBPQT$\cdot$RED^{4+}, the fraction of complexed species (i.e., $\mathbf{2}\subset$CBPQT$\cdot$RED^{4+} and $\mathbf{2}\subset$CBPQT$\cdot$GREEN^{4+}) is expected to be around 35 % at room temperature in the equilibrated MeCN solution. The results obtained (Figure 12c) on the equilibrated solution shows that most of $\mathbf{2}\subset$CBPQT$\cdot$RED^{4+} has been converted into $\mathbf{2}\subset$CBPQT$\cdot$GREEN^{4+} and **2**. The first oxidation potential (+0.42 V) recorded on the equilibrated solution is between those obtained for $\mathbf{2}\subset$CBPQT$\cdot$GREEN^{4+} and **2**, clearly indicating that both $\mathbf{2}\subset$CBPQT$\cdot$GREEN^{4+} and **2** are present in the equilibrium mixture. The limited amount of $\mathbf{2}\subset$CBPQT$\cdot$RED^{4+}, present in the MeCN solution at room temperature is, for example, evidenced by the existence (Figure 12c) of a weak shoulder at the right side of the DPV peak associated with the first oxidation processes.

Conclusion

In conclusion, a bistable, supramolecular species, based on a CBPQT^{4+} ring component which threads onto a semi-dumb-

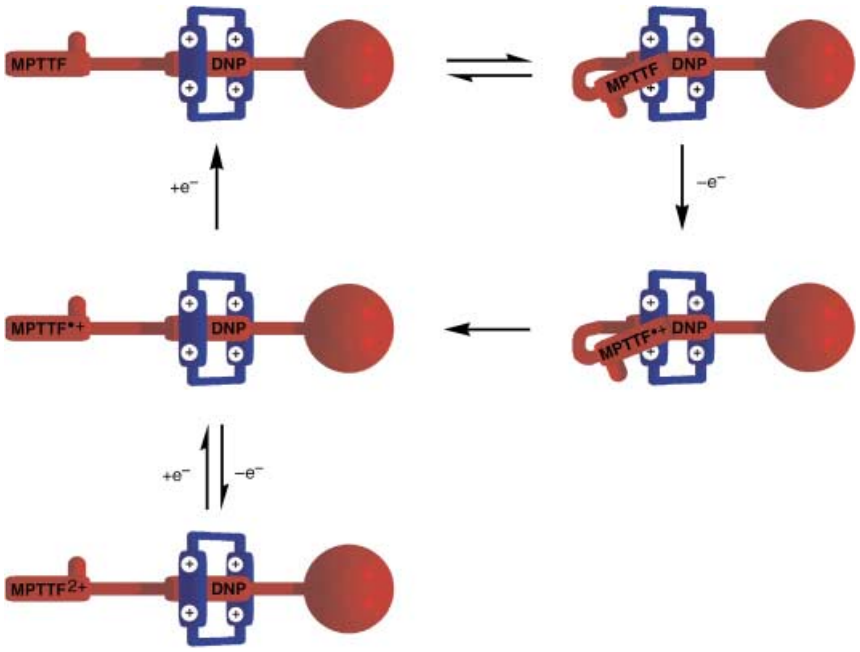

Scheme 3. Schematic representation of the electrochemical behavior of $\mathbf{2}\subset$CBPQT$\cdot$RED^{4+}. For more details, see text.

bell-shaped component containing two different recognition sites—a terminal MPTTF unit and an internal DNP moiety—initially in a fast step to form a kinetically labile [2]pseudorotaxane, which then progresses more slowly to form a second kinetically stable [2]pseudorotaxane, has been characterized. In these [2]pseudorotaxanes the $CBPQT^{4+}$ ring encircles, respectively the MPTTF unit and the DNP moiety. A "speed bump" in the shape of an SMe group has made it possible to isolate the second of the two [2]pseudorotaxanes, suggesting that it has some [2]rotaxane character to it. The presence of the SMe group situated between the two recognition sites in this bistable, supramolecular species made it possible to study the kinetics of the shuttling of the $CBPQT^{4+}$ ring between the two recognition sites. The processes, which are accompanied by detectable color changes, can be followed by ^{1}H NMR and UV/Vis spectroscopies, allowing the kinetic and thermodynamic parameters for the shuttling of $CBPQT^{4+}$ between the MPTTF and DNP recognition sites to be determined in both Me_2CO and MeCN solutions. The passage of $CBPQT^{4+}$ over the SMe group is a significantly faster process in MeCN than it is in Me_2CO at room temperature, an observation which we believe is related to the fact that the passage of $CBPQT^{4+}$ over the SMe group is much more dominated by a loss of entropy in the transition state in Me_2CO. The electrochemical and photophysical investigations show that the [2]pseudorotaxane, in which $CBPQT^{4+}$ encircles the DNP moiety, does not exist as a simple "linear" translational isomer. The data from these investigations suggest that—owing to the length and flexibility of the semi-dumbbell component—the MPTTF unit engages itself "alongside" with one of the bipyridinium units in the $CBPQT^{4+}$ ring in a folded conformation in order to maximize the donor–acceptor interactions. The unique properties of this bistable complex make it an attractive candidate for incorporation into redox-controllable, piston-like, motor-molecules, as well as into other kinds of artificial molecular machinery.[3, 4]

Experimental Section

General methods: Chemicals were purchased from Aldrich and were used as received. The semi-dumbbell compound[13] **2** (Scheme 1), the semi-dumbbell compound[7d, 16] **3** (Scheme 2), and cyclobis(paraquat-*p*-phenylene) tetrakis(hexafluorophosphate)[17] ($CBPQT\cdot 4PF_6$) (Schemes 1 and 2) were all prepared according to literature procedures. Solvents were dried according to literature procedures.[40] Thin-layer chromatography (TLC) was carried out using aluminium sheets pre-coated with silica gel 60F (Merck 5554). The plates were inspected under UV light and, if required, developed in I_2 vapor. Flash column chromatography was carried out using silica gel 60F (Merck 9385, 0.040–0.063 mm). ^{1}H NMR spectra were recorded at 500 MHz on a Bruker Avance500 spectrometer, using residual solvent as the internal standard. All chemical shifts are quoted on a δ scale, and all coupling constants (J) are expressed in Hertz (Hz). Samples were prepared using CD_3COCD_3 or CD_3CN purchased from Cambridge Isotope Labs. Temperatures were calibrated using a neat MeOH sample[41] before or after each experiment and assumed to remain constant during the experiment.

Semi-dumbbell compound 3: ^{1}H NMR (CD_3COCD_3, 500 MHz, 194 K): $\delta = 1.16$ (t, $J = 7.6$ Hz, 3H, CH_2CH_3), 1.26 (s, 18H, $2\times C(CH_3)_3$), 2.47 (s, 3H, SCH_3), 2.55 (q, $J = 7.6$ Hz, 2H, CH_2CH_3), 3.06 (t, $J = 6.6$ Hz, 2H, SCH_2CH_2O), 3.69 (t, $J = 6.6$ Hz, 2H, SCH_2CH_2O), 3.82 (brs, 2H, CH_2O), 4.08 (brs, 2H, CH_2O), 6.90 (d, $J = 8.9$ Hz, 2H, Ar-*H*), 6.93–6.95 (m, 2H, pyrrole-*H*), 7.11–7.19 (m, 10H, Ar-*H*), 7.38 (d, $J = 8.6$ Hz, 4H, Ar-*H*), 10.84 (s, 1H, N*H*).

$CBPQT^{4+}$: ^{1}H NMR (CD_3COCD_3, 500 MHz, 194 K): $\delta = 6.17$ (s, 8H, $4\times CH_2N^+$), 7.95 (s, 8H, Ar-*H*, xylyl), 8.76 (d, $J = 6.5$ Hz, 8H, β-*H*), 9.65 (d, $J = 6.5$ Hz, 8H, α-*H*).

Model system $3\subset CBPQT^{4+}$: Mixing the colorless cyclophane $CBPQT\cdot 4PF_6$ and the yellow semi-dumbbell compound **3** in equimolar proportions in CD_3COCD_3 at room temperature produced a green-colored solution (1.5 mM) and an ^{1}H NMR spectrum (500 MHz) was recorded at 301 K. The exchange between the complexed and free species occurs rapidly (see Figure 5a) on the ^{1}H NMR timescale. Thus, the sample was cooled down to 194 K in order to shift the kinetics into slow exchange which resulted in the appearance of complexed $\mathbf{3}\subset CBPQT^{4+}$ signals exclusively in the spectrum (see Figure 5c), indicating that the complexation of **3** by $CBPQT^{4+}$ is very strong at this temperature. Data for $\mathbf{3}\subset CBPQT^{4+}$: ^{1}H NMR ($CD_3COCD_3$, 500 MHz, 194 K): $\delta = 1.15$ (t, $J = 7.6$ Hz, 3H, CH_2CH_3), 1.25 (s, 18H, $2\times C(CH_3)_3$), 2.56 (q, $J = 7.6$ Hz, 2H, CH_2CH_3), 2.79 (s, 3H, SCH_3), 3.39 (brt, 2H, SCH_2CH_2O), 3.99 (brt, 2H, SCH_2CH_2O), 4.05 (brs, 2H, CH_2O), 4.25 (brs, 2H, CH_2O), 6.05–6.11 (m, 8H, $4\times CH_2N^+$), 6.78–6.81 (m, 2H, pyrrole-*H*), 6.85 (d, $J = 8.7$ Hz, 2H, Ar-*H*), 7.08–7.20 (m, 10H, Ar-*H*), 7.37 (d, $J = 8.5$ Hz, 4H, Ar-*H*), 8.07 (s, 2H, xy-*H*), 8.11 (s, 2H, xy-*H*), 8.19 (s, 2H, xy-*H*), 8.23 (s, 2H, xy-*H*), 8.43 (d, $J = 6.1$ Hz, 2H, β-*H*), 8.48 (d, $J = 6.1$ Hz, 2H, β-*H*), 8.73–8.76 (m, 4H, β-*H*), 9.55 (d, $J = 6.1$ Hz, 2H, α-*H*), 9.59 (d, $J = 6.1$ Hz, 2H, α-*H*), 9.77 (d, $J = 6.1$ Hz, 2H, α-*H*), 9.83 (d, $J = 6.1$ Hz, 2H, α-*H*), 11.00 (s, 1H, N*H*).

Semi-dumbbell compound 2: ^{1}H NMR (CD_3COCD_3, 500 MHz, 194 K): $\delta = 1.15$ (t, $J = 7.6$ Hz, 3H, CH_2CH_3), 1.26 (s, 18H, $2\times C(CH_3)_3$), 2.49 (s, 3H, SCH_3), 2.56 (q, $J = 7.6$ Hz, 2H, CH_2CH_3), 3.11 (t, $J = 6.5$ Hz, 2H, SCH_2CH_2O), 3.82 (t, $J = 6.5$ Hz, 2H, SCH_2CH_2O), 3.99 (brs, 4H, $2\times CH_2O$), 4.04 (brs, 2H, CH_2O), 4.15 (brs, 2H, CH_2O), 4.28 (brs, 4H, $2\times CH_2O$), 6.93 (d, $J = 8.9$ Hz, 2H, Ar-*H*), 6.95–6.97 (m, 2H, pyrrole-*H*), 6.97 (d, $J = 8.2$ Hz, 1H, DNP-*H*-2/6), 6.99 (d, $J = 8.2$ Hz, 1H, DNP-*H*-2/6), 7.11–7.19 (m, 10H, Ar-*H*), 7.36 (t, $J = 8.2$ Hz, 1H, DNP-*H*-3/7), 7.38 (d, $J = 8.6$ Hz, 4H, Ar-*H*), 7.42 (t, $J = 8.2$ Hz, 1H, DNP-*H*-3/7), 7.80 (d, $J = 8.2$ Hz, 1H, DNP-*H*-4/8), 7.83 (d, $J = 8.2$ Hz, 1H, DNP-*H*-4/8), 10.82 (s, 1H, N*H*).

$\mathbf{2}\subset CBPQT\cdot GREEN^{4+}$: A CD_3COCD_3 (1.0 mL) solution of the yellow semi-dumbbell compound **2** (2.2 mg, 2.0 μmol) and a CD_3COCD_3 (1.0 mL) solution of the colorless cyclophane $CBPQT\cdot 4PF_6$ (2.3 mg, 2.1 μmol) were cooled to 195 K (dry ice/Me_2CO). Mixing these two solutions produced a green-colored solution and an ^{1}H NMR spectrum (500 MHz) was recorded at 194 K. Data for $\mathbf{2}\subset CBPQT\cdot GREEN^{4+}$: ^{1}H NMR ($CD_3COCD_3$, 500 MHz, 194 K): $\delta = 1.16$ (t, $J = 7.6$ Hz, 3H, CH_2CH_3), 1.26 (s, 18H, $2\times C(CH_3)_3$), 2.56 (q, $J = 7.6$ Hz, 2H, CH_2CH_3), 2.80 (s, 3H, SCH_3), 3.42 (brt, 2H, SCH_2CH_2O), 4.00 (brs, 2H, CH_2O), 4.04 (brs, 2H, CH_2O), 4.10 (brt, 2H, SCH_2CH_2O), 4.19 (brs, 4H, $2\times CH_2O$), 4.27 (brs, 2H, CH_2O), 4.50 (brs, 2H, CH_2O), 6.03–6.09 (m, 8H, $4\times CH_2N^+$), 6.67–6.69 (m, 2H, pyrrole-*H*), 6.84 (d, $J = 8.1$ Hz, 1H, DNP-*H*-2/6), 6.92 (d, $J = 8.9$ Hz, 2H, Ar-*H*), 6.98 (d, $J = 8.1$ Hz, 1H, DNP-*H*-2/6), 7.03 (t, $J = 8.1$ Hz, 1H, DNP-*H*-3/7), 7.11–7.20 (m, 10H, Ar-*H*), 7.29 (t, $J = 8.1$ Hz, 1H, DNP-*H*-3/7), 7.38 (d, $J = 8.6$ Hz, 4H, Ar-*H*), 7.39 (d, $J = 8.1$ Hz, 1H, DNP-*H*-4/8), 7.59 (d, $J = 8.1$ Hz, 1H, DNP-*H*-4/8), 7.98 (s, 2H, xy-*H*), 8.01 (s, 2H, xy-*H*), 8.17 (s, 2H, xy-*H*), 8.19 (s, 2H, xy-*H*), 8.23 (d, $J = 6.2$ Hz, 2H, β-*H*), 8.25 (d, $J = 6.2$ Hz, 2H, β-*H*), 8.29 (d, $J = 6.2$ Hz, 2H, β-*H*), 8.48 (d, $J = 6.2$ Hz, 2H, β-*H*), 9.39 (d, $J = 6.2$ Hz, 2H, α-*H*), 9.43 (d, $J = 6.2$ Hz, 2H, α-*H*), 9.57 (d, $J = 6.2$ Hz, 2H, α-*H*), 9.72 (d, $J = 6.2$ Hz, 2H, α-*H*), 10.96 (s, 1H, N*H*).

$\mathbf{2}\subset CBPQT\cdot RED^{4+}$: Mixing a solution of the yellow semi-dumbbell compound **2** (15.7 mg, 14.3 μmol) in Me_2CO (10 mL) and the colorless cyclophane $CBPQT\cdot 4PF_6$ (15.7 mg, 14.3 μmol) in Me_2CO (10 mL) produced a green-colored solution immediately. Leaving the green solution to stand for 24 h at room temperature gave a brown solution. The brown solution was subjected to flash column chromatography (silica gel) and the first yellow band containing the semi-dumbbell compound **2** was eluted with Me_2CO, whereupon the eluent was changed to Me_2CO/NH_4PF_6 (1.0 g NH_4PF_6 in 100 mL Me_2CO). The red band was collected to give 15 mL of a solution containing $\mathbf{2}\subset CBPQT\cdot RED^{4+}$. In order to obtain an estimate of the amount of isolated $\mathbf{2}\subset CBPQT\cdot RED^{4+}$, the following assumptions have been made. If it is assumed that the extinction coefficient ε is the same at 400 nm, regardless of whether a solution of $\mathbf{2}\subset CBPQT\cdot RED^{4+}$ or a solution of a 1:1 mixture of the semi-dumbbell compound **2** and $CBPQT^{4+}$ is considered,[42] then the concentration of the isolated Me_2CO solution of

2 ⊂ CBPQT·RED^{4+} can be calculated from a solution of a 1:1 mixture of the semi-dumbbell compound **2** and CBPQT^{4+} with a known concentration. The UV/Vis spectra, shown in Figure 1, were recorded on a 0.72 mM solution of **2** (equal to that of CBPQT^{4+}) and the absorbance at 400 nm was close to 1.36 (295 K) in all cases. The absorbance for the isolated Me_2CO solution of **2** ⊂ CBPQT·RED^{4+} at 400 nm was 0.36 (296 K), a situation which implies that the concentration of **2** ⊂ CBPQT·RED^{4+} was 0.19 mM. Since, the volume of the isolated Me_2CO solution of **2** ⊂ CBPQT·RED^{4+} was 15 mL, the yield of **2** ⊂ CBPQT·RED^{4+} is 6.3 mg (2.9 μmol, 20%). The solvent from the isolated Me_2CO solution—also containing some NH_4PF_6—of **2** ⊂ CBPQT·RED^{4+} was removed in vacuo ($T < 5\,^{\circ}C$), and the resulting red residue was dissolved immediately thereafter in an appropriate solvent (Me_2CO, MeCN, CD_3COCD_3, or CD_3CN). These solutions were stored ready to use at 195 K (dry ice/Me_2CO). Data for **2** ⊂ CBPQT·RED^{4+}: ^{1}H NMR (CD_3COCD_3, 500 MHz, 194 K): $\delta = 1.12$ (t, $J =$ 7.6 Hz, 3H, CH_2CH_3), 1.22 (s, 18H, $2 \times C(CH_3)_3$), 2.53 (q, $J = 7.6$ Hz, 2H, CH_2CH_3), 2.53 (s, 3H, SCH_3), 2.60 (d, $J = 8.1$ Hz, 1H, DNP-*H*-4/8), 2.62 (d, $J = 8.1$ Hz, 1H, DNP-*H*-4/8), 3.48 (br t, 2H, SCH_2CH_2O), 4.17 (br t, 2H, SCH_2CH_2O), 4.34 (br s, 2H, CH_2O), 4.40–4.55 (m, 10H, $5 \times CH_2O$), 5.97 and 6.10 (AB q, $J = 13.2$ Hz, 4H, $2 \times CH_2N^+$), 6.12–6.20 (m, 4H, $2 \times CH_2N^+$), 6.20 (t, $J = 8.1$ Hz, 1H, DNP-*H*-3/7), 6.22 (t, $J = 8.1$ Hz, 1H, DNP-*H*-3/7), 6.34 (d, $J = 8.1$ Hz, 1H, DNP-*H*-2/6), 6.35 (d, $J = 8.1$ Hz, 1H, DNP-*H*-2/6), 6.64 (br s, 1H, pyrrole-*H*), 6.74 (br s, 1H, pyrrole-*H*), 6.95 (d, $J = 8.8$ Hz, 2H, Ar-*H*), 7.08–7.19 (m, 10H, Ar-*H*), 7.33 (d, $J = 8.6$ Hz, 4H, Ar-*H*), 7.63 (d, $J = 6.3$ Hz, 2H, β-*H*), 7.73 (d, $J = 6.3$ Hz, 2H, β-*H*), 7.86 (d, $J = 6.3$ Hz, 2H, β-*H*), 7.88 (d, $J = 6.3$ Hz, 2H, β-*H*), 8.21 (s, 2H, xy-*H*), 8.23 (s, 2H, xy-*H*), 8.43 (s, 2H, xy-*H*), 8.45 (s, 2H, xy-*H*), 9.14 (d, $J = 6.3$ Hz, 2H, α-*H*), 9.19 (d, $J = 6.3$ Hz, 2H, α-*H*), 9.36 (d, $J = 6.3$ Hz, 2H, α-*H*), 9.45 (d, $J = 6.3$ Hz, 2H, α-*H*), 10.69 (s, 1H, N*H*).[43]

Photophysical experiments: All the measurements were performed in air-equilibrated Me_2CO or MeCN solutions. Hexafluorophosphate (PF_6^-) ions were the counterions in the case of all the cationic compounds/complexes. UV/Vis absorption spectra were recorded with a Shimadzu UV-1601PC instrument and the temperature was controlled using a home-made, water-cooled thermostat. The estimated experimental errors are: 2 nm on band maxima and ±5% on the molar absorption coefficients.

Kinetic experiments: The rate constants for the conversion of **2** ⊂ CBPQT·GREEN^{4+} into **2** ⊂ CBPQT·RED^{4+} were measured at different temperatures using UV/Vis spectroscopy as the probe. Experiments were carried out by transferring a Me_2CO solution (1.4 mM) of the semi-dumbbell compound **2** (1.2 mL) and a Me_2CO solution (1.4 mM) of the cyclophane CBPQT·4PF_6 (1.2 mL) to two separate 3.0 mL cuvettes (optical path 1 cm), which subsequently were placed in the thermostatted cell compartment of the UV/Vis spectrophotometer and then allowed to equilibrate to a constant temperature. Then, the two solutions were mixed, affording an equimolar solution (0.72 mM) of **2** and CBPQT^{4+} and the movement of CBPQT^{4+} from the MPTTF to the DNP recognition site was followed using the DNP/CBPQT^{4+} CT band (520 nm) as the probe. The temperature T was measured in the cuvette before and after each experiment and readings of equal to or less than ±0.1 K were obtained. The data points were collected in the early stage of the experiments where the reverse process is not yet occurring to any significant extent and subjected to a first-order analysis by plotting $\ln A/A_0$ against t, where A is the absorbance (at 520 nm) at time t and A_0 is the initial absorbance (at 520 nm). The linear relationship between $\ln A/A_0$ and t was, at each particular temperature, demonstrated by calculation of the correlation coefficient and values (Table 2) of 0.992–0.998 were obtained. The k values were obtained from the slope of these lines, according to the relationship $\ln A/A_0 = -kt$. The estimated experimental errors are ±5%.

The rate constants for the conversion of **2** ⊂ CBPQT·RED^{4+} into **2** ⊂ CBPQT·GREEN^{4+} were measured at different temperatures using UV/Vis spectroscopy as the probe. Experiments were carried out by transferring either a Me_2CO (0.19 mM) or a MeCN (0.10 mM) solution of the stored (dry ice/Me_2CO) **2** ⊂ CBPQT·RED^{4+} to a 3.0 mL cuvette (optical path 1 cm). The cuvette was heated with a heat gun until the temperature of the solution was approximately 285 K, whereupon it was placed in the thermostatted cell compartment of the UV/Vis spectrophotometer and then allowed to adjust to a constant temperature. This procedure took less than 5 min in all cases. The movement of CBPQT^{4+} from the DNP to the MPTTF recognition site was followed using the DNP/CBPQT^{4+} CT band (520 nm) as the probe. The temperature T was measured in the cuvette before and after each experiment and readings of equal to or less than ±0.1 K were obtained. The data points were collected in the early stage of the experiments where the reverse process is not yet occurring to any significant extent and subjected to a first-order analysis by plotting $\ln A/A_0$ against t, where A is the absorbance (at 520 nm) at time t and A_0 is the initial absorbance (at 520 nm). The linear relationship between $\ln A/A_0$ and t was demonstrated at each particular temperature and in every solvent by calculation of the correlation coefficient and values (Tables 3 and 4) of 0.996–1.000 were obtained. The k values were obtained from the slope of these lines, according to the relationship $\ln A/A_0 = -kt$ and the estimated experimental errors are ±5%.

The estimated experimental errors are ±5% for $\Delta G^{\ddagger}$, $\Delta H^{\ddagger}$, and E_a. As a result of the logarithmic nature of the plots and the fact that the $\Delta G^{\ddagger}$ values only have been calculated over an approximate 20 K wide temperature range, the errors in $\Delta S^{\ddagger}$ and A are somewhat larger: we estimate them to be ±25% for $\Delta S^{\ddagger}$ and A.

Electrochemical experiments: Cyclic voltammetric (CV) and differential pulse voltammetric (DPV) experiments were carried out in nitrogen-purged MeCN solutions in a classical three-electrode, single-compartment cell at room temperature. The electrochemical cell was connected to a computerized AutolabPGSTAT10 potentiostat (ECO CHEMIE BV, Utrecht, The Netherlands) controlled by the GPSE software running on a personal computer. The working electrode was a platinum disk electrode and its surface was polished immediately prior to use. The counter electrode was a platinum wire and the reference electrode was a Ag/$AgNO_3$ electrode. 1,1-Dimethylferrocene (+0.31 V vs SCE)[44] was present as an internal standard and all potentials are referenced to the SCE electrode. The concentration of the examined compounds and complexes was 0.1 to 0.2 mM and tetrabutylammonium hexafluorophosphate (0.1M) was added as the supporting electrolyte. All MPTTF derivatives exhibited two pairs of reversible redox waves corresponding to two one-electron processes. The reversibility of the observed processes was established by using the criteria of 1) separation of 60 mV between cathodic and anodic peaks, 2) the close to unity ratio of the intensities of the cathodic and anodic currents, and 3) the constancy of the peak potential on changing sweep rate in the cyclic voltammograms. The same halfwave potentials were obtained from the DPV peaks and from an average of the cathodic and anodic CV peaks, as expected for reversible processes. The experimental errors on the potentials are estimated to be ±10 mV.

Acknowledgement

This research was funded by Carlsbergfondet in Denmark and the Defense Advanced Research Projects Agency (DARPA) in the United States. Some of the compound/complex characterizations were supported by the National Science Foundation under equipment grant no CHE-9974928.

[1] a) J.-M. Lehn, *Supramolecular Chemistry*, VCH, Weinheim, Germany, **1995**; b) *Comprehensive Supramolecular Chemistry*, *Vol. 1–11* (Eds.: J. L. Atwood, J. E. D. Davies, D. D. MacNicol, F. Vögtle, D. Reinhoudt), Pergamon, Oxford, **1996**; c) *Science* **2002**, *295*, 2400–2421 (Viewpoint on Supramolecular Chemistry and Self-Assembly).

[2] a) G. Schill, *Catenanes, Rotaxanes and Knots*, Academic Press, New York, **1971**; b) D. M. Walba, *Tetrahedron* **1985**, *41*, 3161–3212; c) C. O. Dietrich-Buchecker, J.-P. Sauvage, *Chem. Rev.* **1987**, *87*, 795–810; d) H. W. Gibson, H. Marand, *Adv. Mater.* **1993**, *5*, 11–21; e) D. B. Amabilino, J. F. Stoddart, *Chem. Rev.* **1995**, *95*, 2725–2828; f) R. Jäger, F. Vögtle, *Angew. Chem.* **1997**, *109*, 966–980; *Angew. Chem. Int. Ed. Engl.* **1997**, *36*, 930–944; g) G. A. Breault, C. A. Hunter, P. C. Mayers, *Tetrahedron* **1999**, *55*, 5265–5293; h) *Molecular Catenanes, Rotaxanes and Knots* (Eds.: J.-P. Sauvage, C. O. Dietrich-Buchecker), VCH-Wiley, Weinheim, **1999**; i) L. Raehm, D. G. Hamilton, J. K. M. Sanders, *Synlett* **2002**, 1743–1761.

[3] a) M. Gómez-López, J. A. Preece, J. F. Stoddart, *Nanotechnology* **1996**, *7*, 183–192; b) M. D. Ward, *Chem. Ind.* **1997**, 640–645; c) V. Balzani, M. Gómez-López, J. F. Stoddart, *Acc. Chem. Res.* **1998**, *31*, 405–414; d) J.-P. Sauvage, *Acc. Chem. Res.* **1998**, *31*, 611–619; e) A.

Niemz, V. M. Rotello, *Acc. Chem. Res.* **1999**, *32*, 42–52; f) A. E. Kaifer, *Acc. Chem. Res.* **1999**, *32*, 62–71; g) L. Fabbrizzi, M. Licchelli, P. Pallavicini, *Acc. Chem. Res.* **1999**, *32*, 846–853; h) D. A. Leigh, A. Murphy, *Chem. Ind*. **1999**, 178–183; i) M. D. Ward, *Chem. Ind*. **2000**, 22–26; j) V. Balzani, A. Credi, F. M. Raymo, J. F. Stoddart, *Angew. Chem.* **2000**, *112*, 3486–3531; *Angew. Chem. Int. Ed.* **2000**, *39*, 3348–3391; k) R. Ballardini, V. Balzani, A. Credi, M. T. Gandolfi, M. Venturi, *Acc. Chem. Res.* **2001**, *34*, 445–455; l) A. Harada, *Acc. Chem. Res.* **2001**, *34*, 456–464; m) J.-P. Collin, C. Dietrich-Buchecker, P. Gavina, M. C. Jiménez-Molero, J.-P. Sauvage, *Acc. Chem. Res.* **2001**, *34*, 477–487; n) C. Joachim, J. K. Gimzewski, *Struct. Bonding* **2001**, *99*, 1–18; o) T. R. Kelly, J. P. Sestelo, *Struct. Bonding* **2001**, *99*, 19–54; p) J.-P. Sauvage, L. Raehm, *Struct. Bonding* **2001**, *99*, 55–78; q) V. Amendola, L. Fabbrizzi, C. Mangano, P. Pallavicini, *Struct. Bonding* **2001**, *99*, 79–116; r) M. Sano, *Struct. Bonding* **2001**, *99*, 117–140; s) J. Liu, M. Gómez-Kaifer, A. E. Kaifer, *Struct. Bonding* **2001**, *99*, 141–162; t) R. Ballardini, V. Balzani, A. Credi, M. T. Gandolfi, M. Venturi, *Struct. Bonding* **2001**, *99*, 163–188; u) A. R. Pease, J. F. Stoddart, *Struct. Bonding* **2001**, *99*, 189–236; v) A. N. Shipway, E. Katz, I. Willner, *Struct. Bonding* **2001**, *99*, 237–282; w) C. A. Stanier, S. J. Alderman, T. D. W. Claridge, H. L. Anderson, *Angew. Chem.* **2002**, *114*, 1847–1850; *Angew. Chem. Int. Ed.* **2002**, *41*, 1769–1772.

[4] a) J. K. Gimzewski, C. Joachim, R. R. Schlittler, V. Langlais, H. Tang, I. Johannsen, *Science* **1998**, *281*, 531–533; b) T. R. Kelly, H. De Silva, R. A. Silva, *Nature* **1999**, *401*, 150–152; c) N. Koumura, R. W. J. Zijlstra, R. A. van Delden, N. Harada, B. L. Feringa, *Nature* **1999**, *401*, 152–155; d) T. R. Kelly, R. A. Silva, H. De Silva, S. Jasmin, Y. Zhao, *J. Am. Chem. Soc*. **2000**, *122*, 6935–6949; e) B. L. Feringa, R. A. van Delden, N. Koumura, E. M. Geertsema, *Chem. Rev*. **2000**, *100*, 1789–1816; f) C. A. Schalley, K. Beizai, F. Vögtle, *Acc. Chem. Res.* **2001**, *34*, 465–476; g) B. L. Feringa, *Acc. Chem. Res.* **2001**, *34*, 504–513; h) T. R. Kelly, *Acc. Chem. Res.* **2001**, *34*, 514–522; i) N. Koumura, E. M. Geertsema, M. B. van Gelder, A. Meetsma, B. L. Feringa, *J. Am. Chem. Soc.* **2002**, *124*, 5037–5051; j) T. Hugel, N. B. Holland, A. Cattani, L. Moroder, M. Seitz, H. E. Gaub, *Science* **2002**, *296*, 1103–1106.

[5] For investigations relating to a [2]catenane-based, solid-state, electronically reconfigurable, switch, see: a) M. Asakawa, M. Higuchi, G. Mattersteig, T. Nakamura, A. R. Pease, F. M. Raymo, T. Shimizu, J. F. Stoddart, *Adv. Mater*. **2000**, *12*, 1099–1102; b) C. P. Collier, G. Mattersteig, E. W. Wong, Y. Lou, K. Beverly, J. Sampaio, F. M. Raymo, J. F. Stoddart, J. R. Heath, *Science* **2000**, *289*, 1172–1175.

[6] For electronically configurable, molecular-based, logic gates, see: a) C. P. Collier, E. W. Wong, M. Belohradsky, F. M. Raymo, J. F. Stoddart, P. J. Kuekes, R. S. Williams, J. R. Heath, *Science* **1999**, *285*, 391–394; b) E. W. Wong, C. P. Collier, M. Belohradsky, F. M. Raymo, J. F. Stoddart, J. R. Heath, *J. Am. Chem. Soc*. **2000**, *122*, 5831–5840.

[7] a) R. F. Service, *Science* **2001**, *291*, 426–427; b) A. R. Pease, J. O. Jeppesen, J. F. Stoddart, Y. Luo, C. P. Collier, J. R. Heath, *Acc. Chem. Res.* **2001**, *34*, 433–444; c) R. F. Service, *Science* **2001**, *294*, 2442–2443; d) C. P. Collier, J. O. Jeppesen, Y. Luo, J. Perkins, E. W. Wong, J. R. Heath, J. F. Stoddart, *J. Am. Chem. Soc.* **2001**, *123*, 12632–12641; e) Y. Luo, C. P. Collier, J. O. Jeppesen, K. A. Nielsen, E. Delonno, G. Ho, J. Perkins, H.-R. Tseng, T. Yamamoto, J. F. Stoddart, J. R. Heath, *ChemPhysChem* **2002**, *3*, 519–525; f) M. Jacoby, *Chem. Eng. News* **2002**, *80*(39), 38–43; g) Y. Chen, D. A. A. Ohlberg, X. Li, D. R. Stewart, R. S. Williams, J. O. Jeppesen, K. A. Nielsen, J. F. Stoddart, D. L. Olynick, E. Anderson, *Appl. Phys. Lett.* **2003**, *82*, 1610–1612; h) Y. Chen, G.-Y. Jung, D. A. A. Ohlberg, X. Li, D. R. Stewart, J. O. Jeppesen, K. A. Nielsen, J. F. Stoddart, R. S. Williams, *Nanotechnology* **2003**, *14*, 462–468.

[8] a) P.-L. Anelli, N. Spencer, J. F. Stoddart, *J. Am. Chem. Soc*. **1991**, *113*, 5131–5133; b) P.-L. Anelli, P. R. Ashton, R. Ballardini, V. Balzani, M. T. Gandolfi, T. T. Goodnow, A. E. Kaifer, D. Philp, M. Pietraszkiewicz, L. Prodi, M. V. Reddington, A. M. Z. Slawin, N. Spencer, C. Vicent, D. J. Williams, *J. Am. Chem. Soc*. **1992**, *114*, 193–218; c) R. A. Bissell, E. Córdova, A. E. Kaifer, J. F. Stoddart, *Nature* **1994**, *369*, 133–137; d) A. G. Kolchinski, D. H. Busch, N. W. Alcock, *J. Chem. Soc. Chem. Commun*. **1995**, 1289–1291; e) P. R. Ashton, P. T. Glink, J. F. Stoddart, P. A. Tasker, A. J. P. White, D. J. Williams, *Chem. Eur. J.* **1996**, *2*, 729–736; f) N. Solladié, J.-C. Chambron, C. O. Dietrich-Buchecker, J.-P. Sauvage, *Angew. Chem.* **1996**, *108*, 957–960; *Angew. Chem. Int. Ed. Engl.* **1996**, *35*, 906–909; g) P. R. Ashton, R. Ballardini, V. Balzani, M. Belohradsky, M. T. Gandolfi, D. Philp, L. Prodi, F. M. Raymo, M. V. Reddington, N. Spencer, J. F. Stoddart, M. Venturi, D. V. Williams, *J. Am. Chem. Soc.* **1996**, *118*, 4931–4951; h) A. P. Lyon, D. H. Macartney, *Inorg. Chem.* **1997**, *36*, 729–736; i) P.-L. Anelli, M. Asakawa, P. R. Ashton, R. A. Bissell, G. Clavier, R. Górski, A. E. Kaifer, S. J. Langford, G. Mattersteig, S. Menzer, D. Philp, A. M. Z. Slawin, N. Spencer, J. F. Stoddart, M. S. Tolley, D. J. Williams, *Chem. Eur. J.* **1997**, *3*, 1113–1135; j) A. S. Lane, D. A. Leigh, A. Murphy, *J. Am. Chem. Soc.* **1997**, *119*, 11092–11093; k) S. Anderson, R. T. Aplin, T. D. W. Claridge, T. Goodson III, A. C. Maciel, G. Rumbles, J. F. Ryan, H. L. Anderson, *J. Chem. Soc. Perkin Trans. 1* **1998**, 2383–2398; l) A. E. Rowan, P. P. M. Aarts, K. W. M. Koutstaal, *Chem. Commun.* **1998**, 611–612; m) A. G. Kolchinski, N. W. Alcock, R. A. Roesner, D. H. Busch, *Chem. Commun.* **1998**, 1437–1438; n) S. J. Loeb, J. A. Wisner, *Chem. Commun.* **1998**, 2757–2758; o) G. M. Hübner, J. Gläser, C. Seel, F. Vögtle, *Angew. Chem.* **1999**, *111*, 395–398; *Angew. Chem. Int. Ed.* **1999**, *38*, 383–386; p) S. J. Rowan, S. J. Cantrill, J. F. Stoddart, *Org. Lett.* **1999**, *1*, 129–132; q) L. Raehm, J.-M. Kern, J.-P. Sauvage, *Chem. Eur. J.* **1999**, *5*, 3310–3317; r) C. Seel, F. Vögtle, *Chem. Eur. J.* **2000**, *6*, 21–24; s) D. A. Leigh, A. Troisi, F. Zerbetto, *Angew. Chem.* **2000**, *112*, 358–361; *Angew. Chem. Int. Ed*. **2000**, *39*, 350–353; t) S. J. Loeb, J. A. Wisner, *Chem. Commun.* **2000**, 845–846; u) K. Chichak, M. C. Walsh, N. R. Branda, *Chem. Commun.* **2000**, 847–848; v) J. E. H. Buston, J. R. Young, H. L. Anderson, *Chem. Commun.* **2000**, 905–906; w) S. J. Cantrill, D. A. Fulton, A. M. Heiss, A. R. Pease, J. F. Stoddart, A. J. P. White, D. J. Williams, *Chem. Eur. J.* **2000**, *6*, 2274–2287; x) S.-H. Chiu, J. F. Stoddart, *J. Am. Chem. Soc.* **2002**, *124*, 4174–4175; y) J. A. Wisner, P. D. Beer, M. G. B. Drew, M. R. Sambrook, *J. Am. Chem. Soc.* **2002**, *124*, 12469–12476; z) S.-H. Chiu, S. J. Rowan, S. J. Cantrill, J. F. Stoddart A. J. P. White, D. J. Williams, *Chem. Eur. J.* **2002**, *8*, 5170–5183.

[9] The "slippage" methodology was first exploited for the rotaxane syntheses that were conducted in a statistical manner. For examples, see: a) I. T. Harrison, *J. Chem. Soc. Chem. Commun.* **1972**, 231–232; b) G. Schill, W. Beckmann, N. Schweikert, H. Fritz, *Chem. Ber.* **1986**, *119*, 2647–2655. A successful template-directed synthesis of rotaxanes utilizing slippage was reported in 1993. See: c) P. R. Ashton, M. Belohradsky, D. Philp, J. F. Stoddart, *J. Chem. Soc. Chem. Commun.* **1993**, 1269–1274. For other examples, see: d) ref. [8g]; e) M. Händel, M. Plevoets, S. Gestermann, F. Vögtle, *Angew. Chem.* **1997**, *109*, 1248–1250; *Angew. Chem. Int. Ed. Engl.* **1997**, *36*, 1199–1201; f) F. M. Raymo, K. N. Houk, J. F. Stoddart, *J. Am. Chem. Soc.* **1998**, *120*, 9318–9322; g) M. C. T. Fyfe, F. M. Raymo, J. F. Stoddart, in *Stimulating Concepts in Chemistry* (Eds.: M. Shibasaki, J. F. Stoddart, F. Vögtle), VCH-Wiley, Weinheim, **2000**, pp. 211–220.

[10] P. R. Ashton, I. Baxter, M. C. T. Fyfe, F. M. Raymo, N. Spencer, J. F. Stoddart, A. J. P. White, D. J. Williams, *J. Am. Chem. Soc.* **1998**, *120*, 2297–2307.

[11] The distinction between rotaxanes and pseudorotaxanes is far from being a straightforward one. When size-complementarity between the stoppers and the macrocyclic component is achieved, certain "rotaxanes" behave as pseudorotaxanes and can dissociate into their constituent components under appropriate conditions. Thus, a species which is a rotaxane at ambient temperature might well be a pseudorotaxane at elevated temperatures. Even a solvent change can turn a rotaxane into a pseudorotaxane at the same temperature. See: a) F. M. Raymo, J. F. Stoddart, *Chem. Rev.* **1999**, *99*, 1643–1663; b) S.-H. Chiu, S. J. Rowan, S. J. Cantrill, P. T. Glink, R. L. Garrell, J. F. Stoddart, *Org. Lett.* **2000**, *2*, 3631–3634; c) A. Affeld, G. M. Hübner, C. Seel, C. A. Schalley, *Eur. J. Org. Chem.* **2001**, 2877–2890.

[12] For a preliminary communication describing parts of this work, see: J. O. Jeppesen, J. Becher, J. F. Stoddart, *Org. Lett.* **2002**, *4*, 557–560.

[13] a) J. O. Jeppesen, J. Perkins, J. Becher J. F. Stoddart, *Angew. Chem.* **2001**, *113*, 1256–1261; *Angew. Chem. Int. Ed.* **2001**, *40*, 1216–1221; b) J. O. Jeppesen, K. A. Nielsen, J. Perkins, S. A. Vignon, A. Di Fabio, R. Ballardini, M. T. Gandolfi, M. Venturi, V. Balzani, J. Becher, J. F. Stoddart, *Chem. Eur. J.* **2003**, *9*, 2982–3007.

[14] a) D. Philp, A. M. Z. Slawin, N. Spencer, J. F. Stoddart, D. J. Williams, *J. Chem. Soc. Chem. Commun.* **1991**, 1584–1586; b) W. Devonport,

M. A. Blower, M. R. Bryce, L. M. Goldenberg, *J. Org. Chem*. **1997**, *62*, 885 – 887; c) M. B. Nielsen, J. O. Jeppesen, J. Lau, C. Lomholt, D. Damgaard, J. P. Jacobsen, J. Becher, J. F. Stoddart, *J. Org. Chem.* **2001**, *66*, 3559 – 3563.

[15] a) P. R. Ashton, R. Ballardini, V. Balzani, S. E. Boyd, A. Credi, M. T. Gandolfi, M. Gómez-López, S. Iqbal, D. Philp, J. A. Preece, L. Prodi, H. G. Ricketts, J. F. Stoddart, M. S. Tolley, M. Venturi, A. J. P. White, D. J. Williams, *Chem. Eur. J.* **1997**, *3*, 152 – 170; b) A. Credi, M. Montalti, V. Balzani, S. J. Langford, F. M. Raymo, J. F. Stoddart, *New J. Chem.* **1998**, *22*, 1061 – 1065.

[16] J. O. Jeppesen, J. Perkins, J. Becher, J. F. Stoddart, *Org. Lett.* **2000**, *2*, 3547 – 3550.

[17] M. Asakawa, W. Dehaen, G. L′abbé, S. Menzer, J. Nouwen, F. M. Raymo, J. F. Stoddart, D. J. Williams, *J. Org. Chem*. **1996**, *61*, 9591 – 9595.

[18] The ΔG° values were calculated using the relationship $\Delta G^{\circ} = \Delta RT\ln K_a$ where R is the gas constant and T is the absolute temperature.

[19] a) R. Wolf, M. Asakawa, P. R. Ashton, M. Gómez-López, C. Hamers, S. Menzer, I. W. Parsons, N. Spencer, J. F. Stoddart, M. S. Tolley, D. J. Williams, *Angew. Chem.* **1998**, *110*, 1018 – 1022; *Angew. Chem. Int. Ed.* **1998**, *37*, 975 – 979; b) V. Balzani, A. Ceroni, A. Credi, M. Gómez-López, C. Hamers, J. F. Stoddart, R. Wolf, *New J. Chem.* **2001**, *25*, 25 – 31.

[20] For further details, see the Experimental Section.

[21] The presence of folded conformations wherein the MPTTF unit enters into an "alongside" interaction with the $CBPQT^{4+}$ ring has previously been observed in both bistable [2]rotaxanes and [2]pseudorotaxanes incorporating an MPTTF unit and a DNP moiety on the rod-section of its dumbbell component, see: ref. [13b].

[22] A little contribution might also arise from the tail of the DNP/$CBPQT^{4+}$ CT absorption band in $\mathbf{2}\subset CBPQT\cdot RED^{4+}$, but the ε value for this interaction is normally very weak at wavelengths higher than 700 nm.

[23] The rate of complexation/decomplexation for $CBPQT^{4+}$ with **3** was determined by partial line shape analysis of the SMe signals for the complexed and uncomplexed forms. The chemical shifts, line widths and integrations were used as input and determined from the low temperature spectrum where no exchange is observed. Simulation of the spectrum using the Spinworks program (Spinworks Version 1.3, K, Marat, University of Manitoba, Department of Chemistry) at 247 K gave a k_{uc} value of 425 s^{-1} corresponding to a $\Delta G_{uc}^{\ddagger}$ value of 11.4 ± 0.1 kcal mol^{-1}. The corresponding value for complexation can be calculated by subtracting ΔG° for the complexed versus uncomplexed forms ($\approx$0.3 kcal mol^{-1}) to give a $\Delta G_{c}^{\ddagger}$ value of 11.1 ± 0.1 kcal mol^{-1}.

[24] An SMe group attached to an MPTTF unit reveals significant changes in its chemical shift when the MPTTF unit is located "inside" the $CBPQT^{4+}$ ring. Such an SMe group resonates at a chemical shift higher than δ 2.6, whereas an "uncomplexed" SMe group has a chemical shift of about δ 2.40 ppm. See: a) ref. [13]; b) ref. [16].

[25] See Supporting Information.

[26] a) M. Asakawa, P. R. Ashton, V. Balzani, C. L. Brown, A. Credi, O. A. Matthews, S. P. Newton, F. M. Raymo, A. N. Shipway, N. Spencer, A. Quick, J. F. Stoddart, A. J. P. White, D. J. Williams, *Chem. Eur. J.* **1999**, *5*, 860 – 875; b) ref. [13b]; c) ref. [15a].

[27] The solutions, containing initially a 1:1 mixture of **2** and $CBPQT^{4+}$, were allowed to stand at room temperature for 48 h before ^{1}H NMR spectra (500 MHz, 273 K) were recorded. Subsequently, the ratios between $\mathbf{2}\subset CBPQT\cdot GREEN^{4+}$ and $\mathbf{2}\subset CBPQT\cdot RED^{4+}$ were determined by integration of the resonances associated with SMe protons in $\mathbf{2}\subset CBPQT\cdot GREEN^{4+}$ and $\mathbf{2}\subset CBPQT\cdot RED^{4+}$, respectively.

[28] K. J. Laidler, *Chemical Kinetics*, Harper Collins Publisher, New York, **1987**.

[29] At each temperature, first-order kinetics are observed to be obeyed, i.e., good straight lines are observed (see Tables 2 – 4 and Supporting Information) when $\ln A/A_0$ is plotted against t, where A is the absorbance (at 520 nm) at time t and A_0 is the initial absorbance (at 520 nm). This outcome is a consequence of the fact that the data points were collected in the early stage of the experiments where the reverse process is not yet occurring to any significant extent.

[30] The $\Delta G^{\ddagger}$ values were calculated using the relationship $\Delta G^{\ddagger} = -RT\ln(kh/k_BT)$, where R is the gas constant, T is the absolute temperature, k is the rate constant, h is Planck's constant and k_B is the Boltzmann constant.

[31] In fact, we tried to use the absorbance at 800 nm as a probe for monitoring the decrease in the concentration of $\mathbf{2}\subset CBPQT\cdot GREEN^{4+}$ in Me_2CO and a first-order kinetic treatment of the data gave a good linear relationship between $\ln A/A_0$ and t. However, at all temperatures probed, the k values obtained from the above experiments were substantially lower than those obtained using the DNP/$CBPQT^{4+}$ CT band at 520 nm as a probe, clearly indicating that the MPTTF unit's "alongside" interaction with $CBPQT^{4+}$ in $\mathbf{2}\subset CBPQT\cdot RED^{4+}$ interferes with the MPTTF unit's "inside" interaction in $\mathbf{2}\subset CBPQT\cdot GREEN^{4+}$.

[32] The kinetics of the shuttling of $CBPQT^{4+}$ from the MPTTF to the DNP recognition site in $\mathbf{2}\subset CBPQT^{4+}$ have also been investigated using ^{1}H NMR spectroscopy. Immediately after mixing equimolar amounts of $CBPQT^{4+}$ and **2** in CD_3COCD_3 (1.0 mM) an ^{1}H NMR spectrum (500 MHz) was recorded at 301 K and the shuttling of $CBPQT^{4+}$ from the MPTTF recognition site in $\mathbf{2}\subset CBPQT^{4+}$ to the DNP recognition site was followed in the early stage of the experiment where the reverse process is not yet occurring to any significant extent using the SMe resonance in $\mathbf{2}\subset CBPQT\cdot RED^{4+}$ and $\mathbf{2}\subset CBPQT\cdot GREEN^{4+}$ as probes. A rate constant of 2.6×10^{-5} s^{-1} at 301 K for the slippage of $CBPQT^{4+}$ over the SMe group, in the direction from GREEN to RED, was obtained from the slope of a plot (see Supporting Information) of $\ln[I_{SMe,GREEN})/(I_{SMe,GREEN}+I_{SMe,RED})]$ against t, where $I_{SMe,GREEN}$ and $I_{SMe,RED}$ denotes the integrals of the SMe resonance for $\mathbf{2}\subset CBPQT\cdot GREEN^{4+}$ and $\mathbf{2}\subset CBPQT\cdot RED^{4+}$, respectively, and t the time.

[33] The kinetics of the shuttling of $CBPQT^{4+}$ from the DNP recognition site to the MPTTF recognition site in the bistable [2]rotaxane $\mathbf{1}^{4+}$ have previously (see: ref. [13]) been investigated using ^{1}H NMR spectroscopy and a rate constant of 2.3×10^{-5} s^{-1} for the slippage of $CBPQT^{4+}$ over the SMe group, in the direction from $\mathbf{1}\cdot RED^{4+}$ to $\mathbf{1}\cdot GREEN^{4+}$, was obtained in CD_3CDCD_3 at 300 K.

[34] An inspection of the data recorded in Table 5 reveals that the $\Delta G^{\ddagger}$ values for "GREEN to RED" and "RED to GREEN" show a small difference, with the "RED to GREEN" value being slightly larger. On account of the fact that the "GREEN" isomer is thermodynamically lower in energy than the "RED" isomer, one would expect the opposite ordering of $\Delta G^{\ddagger}$ values. In this case, however, the two values reported are essentially the same within experimental error. This discrepancy is most likely a result of minor variations between the two experiments, as the difference in $\Delta G^{\ddagger}$ values would be expected to be small.

[35] a) P. R. Ashton, R. Ballardini, V. Balzani, A. Credi, M. T. Gandolfi, D. J.-F. Marquis, L. Pérez-Garcia, L. Prodi, J. F. Stoddart, M. Venturi, A. J. P. White, D. J. Williams, *J. Am. Chem. Soc.* **1995**, *117*, 11171 – 11197; b) M. Asakawa, P. R. Ashton, R. Ballardini, V. Balzani, M. Belohradsky, M. T. Gandolfi, O. Kocian, L. Prodi, F. M. Raymo, J. F. Stoddart, M. Venturi, *J. Am. Chem. Soc.* **1997**, *119*, 302 – 310; c) R. Ballardini, V. Balzani, W. Dehaen, A. E. Dell'Erba, F. M. Raymo, J. F. Stoddart, M. Venturi, *Eur. J. Org. Chem*. **2000**, 591 – 602.

[36] V. Balzani, A. Credi, G. Mattersteig, O. A. Matthews, F. M. Raymo, J. F. Stoddart, M. Venturi, A. J. P. White, D. J. Williams, *J. Org. Chem*. **2000**, *65*, 1924 – 1936.

[37] In a 0.1 mM MeCN solution, containing equimolar amounts of $CBPQT^{4+}$ and **3**, the fraction of the [2]pseudorotaxane $\mathbf{3}\subset CBPQT^{4+}$ is only 35 %.

[38] a) M. Asakawa, P. R. Ashton, V. Balzani, A. Credi, G. Mattersteig, O. A. Matthews, N. Montalti, N. Spencer, J. F. Stoddart, M. Venturi, *Chem. Eur. J.* **1997**, *3*, 1992 – 1996; b) M. Asakawa, P. R. Ashton, V. Balzani, S. E. Boyd, A. Credi, G. Mattersteig, S. Menzer, M. Montalti, F. M. Raymo, C. Ruffilli, J. F. Stoddart, M. Venturi, D. J. Williams, *Eur. J. Org. Chem.* **1999**, 985 – 994.

[39] Assuming that the K_a value for the complexation of $CBPQT^{4+}$ with **2** is not less than 8800 M^{-1}, then the fraction of the [2]pseudorotaxane $\mathbf{2}\subset CBPQT^{4+}$ is at least 94 % in a MeCN solution containing 0.2 mM of **2** and 10 equivalents of $CBPQT^{4+}$.

[40] D. D. Perrin, W. L. F. Armarego, *Purification of Laboratory Chemicals*, Pergamon Press, New York, **1988**.

[41] A. L. Van Geet, *Anal. Chem.* **1970**, *42*, 679–680.
[42] Such an assumption is reasonable, since—as is evidenced from an inspection of Figures 1 and 3, a solution of a 1:1 mixture of **2** and $CBPQT^{4+}$ or a solution of $\mathbf{2} \subset CBPQT \cdot RED^{4+}$ has almost a "constant" absorbance at 400 nm.
[43] The appearance of NH_4^+ in the isolated $\mathbf{2} \subset CBPQT \cdot RED^{4+}$ is evident from a triplet (intensity: 1:1:1) resonating at δ 7.62 in the ^{1}H NMR spectrum.
[44] S. F. Nelsen, L.-J. Chen, M. T. Ramm, G. T. Voy, D. R. Powell, M. A. Aceola, T. R. Seehafer, J. J. Sabelko, J. R. Pladziewicz, *J. Org. Chem.* **1996**, *61*, 1405–1412.

Received: January 31, 2003 [F4798]

